Universidade do Minho
Escola de Medicina

Andreia Raquel Pereira Nunes

Targeting cancer cell metabolism using targeted drug delivery systems

Desenvolvimento de nanossistemas para a inibição do metabolismo celular tumoral

setembro de 2018

Targeting cancer cell metabolism using targeted drug delivery systems
Desenvolvimento de nanossistemas para a inibição do metabolismo celular tumoral
Andreia Raquel Pereira Nunes
UMinho|2018

Universidade do Minho
Escola de Medicina

Andreia Raquel Pereira Nunes

Targeting cancer cell metabolism using targeted drug delivery systems

Desenvolvimento de nanossistemas para a inibição do metabolismo celular tumoral

Dissertação de Mestrado
Mestrado em Ciências da Saúde

Trabalho efetuado sob a orientação da
Doutora Sara Costa Granja
e da
Professora Doutora Maria de Fátima Monginho Baltazar

setembro de 2018

Agradecimentos

À Doutora Sara Granja, por tudo! Por teres acreditado e apostado em mim para a realização deste projeto e por tudo que daí em diante desabrochou. Obrigada por me teres feito crescer quer como profissional quer como pessoa e, acima de tudo, por me fazeres evoluir enquanto investigadora. Obrigada por toda a paciência, por todo o apoio, por toda a insistência e por nunca teres desistido de mim e do nosso projeto.

"*A persistência é o caminho do êxito.*" – Charles Chaplin

À Professora Doutora Fátima Baltazar, pela oportunidade em realizar este projeto sob sua orientação. Gostaria de lhe agradecer pelo apoio prestado, pelas suas sugestões e por toda a simpatia.

"*A diferença entre o possível e o impossível está na vontade humana.*" – Pasteur

À Doutora Helena Ferreira e ao Doutor Nuno Neves, pela vossa contribuição no desenvolvimento das nanopartículas e por levarem este trabalho de investigação avante. Por toda a simpatia e por toda a atenção em esclarecem todas as dúvidas que surgiram durante o progresso deste projeto.

"*Toda a conquista começa com a decisão de tentar.*" – Gail Devers

A todos os investigadores do domínio das Ciências Cirúrgicas que, de uma forma ou de outra, contribuíram para o desenvolvimento desta tese. Obrigada por toda a ajuda e apoio e por todos os bons momentos que passamos juntos.

"*Somos todos anjos de uma só asa, e só podemos voar quando nos abraçamos uns aos outros.*" – Fernando Pessoa

Aos professores/investigadores e funcionários do ICVS e da Escola de Medicina pela simpatia e pelo conhecimento partilhado. À Comissão de Mestrado pela oportunidade para a realização desta tese.

"O sucesso é a soma de pequenos esforços repetidos dia após dia." – Robert Collier

Às minhas três plebes (ML, NF e SC), que fizeram com que este sonho se tornasse realidade. Se cheguei até aqui foi graças a vocês e devo-vos muito por isso! Vocês foram, sem dúvida, o meu maior pilar durante este ano e vou-vos levar comigo "para a vida toda". Obrigada por me acolherem no vosso coração gigante!

"*You're my best friend, the one that I'll love until the end.*" – Richie Campbell

Às minhas colegas de casa, por fazerem dos meus finais de dia algo especial. Obrigada por terem estado presentes quer nos bons ou maus momentos e por nunca me deixarem vacilar. Obrigada por todo apoio e por alegrarem o meu dia. Não me irei esquecer dos vossos crepes e dos vossos cappuccinos.

"*Aqueles que passam por nós, não vão sós, não nos deixam sós. Deixam um pouco de si, levam um pouco de nós.*" – Antoine de Saint-Exupéry

Aos meus amigos: aos de Barcelos, aos da licenciatura, aos do Nico Dance Studio, e a todos os outros que representam uma parte de mim. Vocês foram peças fundamentais neste caminho. Obrigada pela força, pelas palavras certas e pela coragem que me transmitiram.

"*Nenhum caminho é longo demais quando um amigo nos acompanha.*" – Ralph Waldo Emerson

Às cinco flores que crescem em mim: aos avozinhos, à minha mamacita, ao Paulo e à minha pequeninha; por toda a preocupação, por todos os conselhos, pelo incentivo e acima de tudo por todo o amor e carinho. Obrigada por toda a magia que dão à minha vida, por fazerem o meu mundo girar e por tornarem o meu sorriso cada vez maior. Obrigada por proporcionarem a concretização deste sonho!

"*The earth laughs in flowers.*" – Ralph Waldo Emerson

À minha restante família, por toda a preocupação, apoio e carinho. Obrigada pelo incentivo e pela coragem que sempre me transmitiram. Obrigada por estarem sempre presentes durante esta viagem e por fazerem de mim aquilo que me tornei hoje!

"*You don't choose your family. They are god's gift to you, as you are to them.*" – Desmond Tutu

The work presented in this thesis was performed in the Surgical Sciences Research Domain in the Life and Health Sciences Research Institute (ICVS), School of Medicine, University of Minho, Braga, Portugal (ICVS/3B´S-PT Government Associate Laboratory Braga/Guimarães, Portugal). Financial support was provided by FEDER funds through the Operational Programme Competitiveness Factors - COMPETE and National Funds through FCT - Foundation for Science and Technology under the project POCI-01-0145-FEDER-007038; and by the project NORTE-01-0145-FEDER-000013, supported by Norte Portugal Regional Operational Programme (NORTE 2020), under the PORTUGAL 2020 Partnership Agreement, through the European Regional Development Fund (ERDF).

"Para ser grande, sê inteiro.

Nada teu exagera ou exclui.

Sê todo em cada coisa.

Põe quanto és no mínimo que fazes.

Assim em cada lago a lua toda brilha,

Porque alta vive" – Ricardo Reis

Summary

Targeting cancer cell metabolism using targeted drug delivery systems

Lung cancer is the leading cause of cancer mortality in the world. Resistance to conventional therapies remains a hindrance for patient's treatment. Therefore, it is crucial to develop more effective anti-cancer strategies. Solid tumors are characterized by an exorbitant glycolytic phenotype even in high oxygen tension, which leads to an enhanced production of lactate and consequently, its efflux to the tumor microenvironment through monocarboxylate transporters (MCTs). MCT1, MCT4 and their chaperone CD147 are overexpressed in tumor malignancies and their high levels were correlated with tumor growth, invasion and metastasis. Published results from our laboratory revealed that CD147 knock-out decreased lactate export in lung cancer cells and sensitized tumor cells to phenformin, a mitochondrial inhibitor, observing a drastic decrease in cell growth *in vitro* and tumor growth *in vivo*. In this study, we envision the development of CD147-targeted liposomes carrying phenformin and characterize its efficacy to eliminate cancer cells. Our data showed that free phenformin decreased 2D and 3D-cell growth in lung cancer cells. The antibody against CD147 that we tested did not impair lactate efflux, however it reduced cell migration and invasion. Moreover, the treatment with large unilamellar liposomes (LUVs) carrying phenformin decreased 2D and 3D-cell growth and increased lactate production. Importantly, we confirmed that anti-CD147 LUVs carrying phenformin were internalized by tumor cells. In summary, we demonstrated that anti-CD147 liposomes carrying phenformin could compromise the growth and aggressiveness of lung cancer cells. With this study, we expect to unveil new strategies to target tumor metabolism and provide an effective therapy for lung cancer, however, further experiments are still needed.

Resumo

Desenvolvimento de nanossistemas para a inibição do metabolismo celular tumoral

As neoplasias pulmonares são uma das principais causas de morte por cancro em todo o mundo. A resistência aos tratamentos convencionais continua a ser um entrave para o tratamento dos pacientes. Deste modo, torna-se crucial o desenvolvimento de terapias anticancerígenas mais eficazes. Os tumores sólidos são caracterizados por um exorbitante fenótipo glicolítico mesmo na presença de elevadas concentrações de oxigénio, o que conduz a uma elevada produção de lactato e, consequentemente, ao seu exporte para o microambiente tumoral, através de transportadores de monocarboxilatos (MCTs). O MCT1, o MCT4 e a sua chaperona, CD147, estão sobre-expressos em tumores malignos, sendo que, elevados níveis destas proteínas foram associados ao crescimento e à invasão tumoral e à formação de metástases. Resultados publicados pelo nosso laboratório demonstraram que o *knock-out* da CD147 diminuiu o exporte de lactato em células de cancro de pulmão e sensibilizou-as para o efeito da fenformina, um inibidor mitocondrial, tendo-se observado uma drástica diminuição no crescimento celular *in vitro* e no crescimento tumoral *in vivo*. Deste modo, este projeto de investigação tem como objetivo principal o desenvolvimento de lipossomas incorporados com fenformina tendo como alvo a CD147, e a caracterização da sua eficácia para eliminar células cancerígenas. Os resultados deste estudo mostraram que a fenformina foi capaz de diminuir o crescimento de linhas de cancro do pulmão em culturas celulares a duas e três dimensões. O anticorpo anti-CD147 testado não comprometeu o efluxo de lactato, contudo, reduziu a migração e a invasão celular. Para além disso, o tratamento com lipossomas incorporados com fenformina diminuiu o crescimento celular a duas e três dimensões e aumentou a produção de lactato. Mais importante, as células tumorais internalizaram lipossomas incorporados com fenformina e anticorpo anti-CD147. Em suma, demonstramos que lipossomas incorporados com fenformina e anticorpo anti-CD147 podem comprometer o crescimento e agressividade das células de cancro do pulmão. Com este estudo, pretendemos desenvolver novas estratégias com alvo no metabolismo tumoral, promovendo uma terapia mais eficaz para o cancro do pulmão, contudo, mais estudos serão necessários.

Contents

Abbreviation List

3PG	3-Phosphoglycerate
AC	Adenocarcinoma
ALK	Anaplastic Lymphoma Kinase
AMPK	AMP-Activated Protein Kinase
ATCC	American Type Culture Collection
BSA	Bovine Serum Albumin
BSG	Basigin
CD147	Cluster of Differentiation 147
CHC	α-Cyano-4-Hydroxycinnamate
CREB	cAMP-Response Element-Binding Protein
CTLA-4	T-Lymphocyte Associated Antigen 4
DAPI	4',6-diamidino-2-phenylindole
DBDS	4,4-O-dibenzamidostilbene-2,2O-disulphonate
DIDS	4,4-Odiisothiocyanostilbene-2,20-disulphonate
DMEM	Dulbecco's Modified Eagle Medium
DSPE-PEG2000	poly(ethyleneglycol)(2000)-distearyl phosphatidylethanolamine
EGF	Epidermal Growth Factor
EGFR	Epithelial Growth Factor Receptor
EGR2	Early Growth Response Protein 2
EMT	Epithelial-Mesenchymal Transition
EMMPRIN	Extracellular Matrix Metalloproteinase Inducer
ERK 1/2	Extracellular-Signal Related Kinase
F6P	Fructose-6-Phosphate
FAK	Focal Adhesion Kinase
FBS	Fetal Bovine Serum
FDA	Food and Drug Administration
G6P	Glucose-6-Phosphate
GA3P	Glyceraldehyde-3-Phosphate
HA	Hyaluronan
HHC	Human Hepatoma Cells
HIF1-α	Hypoxia Inducible Factor 1-α
IARC	International Agency for Research on Cancer
IC_{50}	Half Maximal Inhibitory Concentration
IFN-γ	Interferon-γ
Ig	Immunoglobulin
LCC	Large Cell Carcinoma

LUV	Large Unilamellar Vesicle
mAb	Monoclonal Antibody
MCT	Monocarboxylate Transporter
MMP	Matrix Metalloproteinase
mTOR	Mammalian Target of Rapamycin
NF-κβ	Nuclear Factor κ-light Chain-Enhancer of Activated B Cells
NSCLC	Non-Small Cell Lung Cancer
OXPHOS	Oxidative Phosphorylation
pCMBS	*p*-Chlomercuribenzene Sulfonate
PD-1	Programmed Cell-Death 1
PEG	Polyethylene Glycol
PPP	Pentose Phosphate Pathway
Ribose-5P	Ribose-5-Phosphate
ROS	Reactive Species of Oxygen
SCC	Squamous-cell Carcinoma
SCLC	Small Cell Lung Cancer
SLC16A	Solute Carrier family 16
Sp 1/3	Specific Proteins 1/3
SRB	Sulphorhodamine B
TCA	Trichloroacetic Acid
TGF-β	Transforming Growth Factor β
TM	Transmembrane
TMB	Tetramethyl-Benzidine
TNF-α	Tumor Necrosis Factor α
TSH	Thyroid-Stimulating Hormone
TSNAs	Tobacco-specific N-nitrosamines
VEGF	Vascular Endothelial Growth Factor

List of Figures

List of Tables

Chapter 1

INTRODUCTION

1. INTRODUCTION

1.1 Cancer incidence and mortality: an overview

Cancer is a leading cause of mortality worldwide[1]. The global burden of cancer is rising in high developed countries but especially in low and middle-income countries[2]. The GLOBOCAN 2012 estimated 14.1 million new cancer cases, 8.2 million cancer deaths and 32.6 million people living with cancer in 2012 worldwide. Despite all the efforts concerning cancer therapies, an increase to 21.6 million patients a year is projected for 2030. Lung (13%), breast (12%), colon-rectum (9.7%), prostate (7.8%), stomach (6.8%) and liver (5.6%) cancers were identified as the most six common types being lung, liver and stomach cancers associated with a higher percentage of cancer-related deaths (Figure 1.1)[3,4].

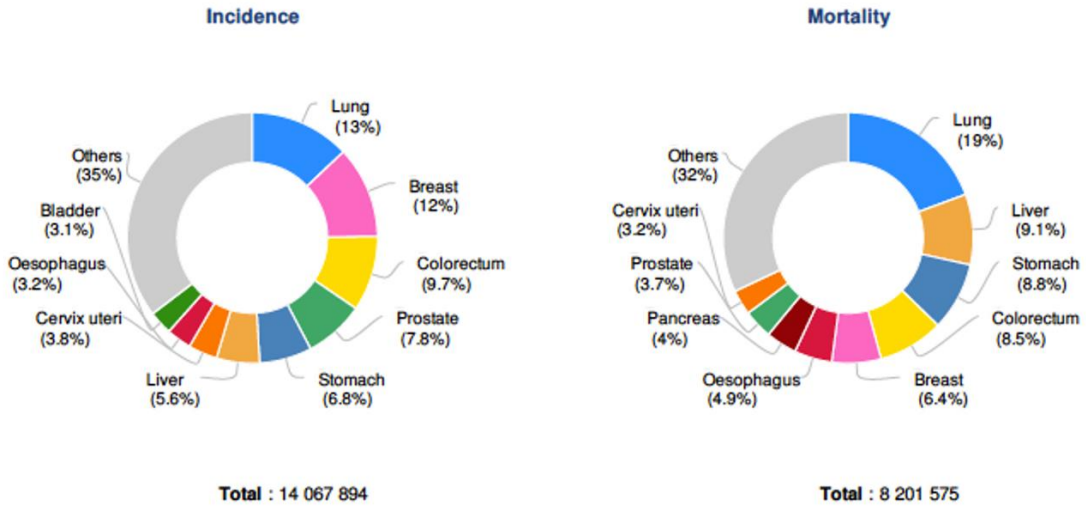

Figure 1.1. Estimated percentages of incidence (right) and mortality (left) cases worldwide in 2012, according to the International Agency for Research on Cancer (IARC). Adapted from Globocan, 2018, http://gco.iarc.fr/.

1.2 Lung cancer

1.2.1 Epidemiology

Lung cancer was identified as the most commonly diagnosed and the most fatal cancer in the last decades, with a 5-year survival rate less than 15%. In 2012, it was estimated 1.8 million new cases of which 58% occurred in less developed countries. In turn, approximately 1.6 million deaths were estimated at the same year having been foreseen a global increase of 86% until 2035. The world incidence rate of lung carcinoma between genders is different due to distinctive smocking prevalence trends, afflicting more men (16.7% of the total) than women (8.7%). Among men the highest estimated age-standardized incidence rates were found in Central and East Europe (53.5 per 100.000) and Eastern Asia (50.4) and the lowest rates in Middle and Western Africa (2 and 1.7, respectively). In women, the geographic pattern is quite different, being Northern America (33.8), Northern Europe (23.7) and Eastern Asia (19.2), the regions with higher number of lung cancer cases and Western and Middle Africa (1.1 and 0.8, respectively) with the lower number of cases[5–7]. In Portugal, the oncologic registers from 2010 identified lung cancer as the 3rd most common cancer (incidence rate= 35.8 per 100.000) being one of the cancers most associated with mortality (34.5 per 100.000). Specifically, the coastal zone of mainland Portugal and the autonomous region of Azores were identified as the regions with higher number of lung cancer cases for both genders. In accordance with the global trends, lung cancer was more frequent in men than women, however the number of new cases is now decreasing in men whereas, in women, the incidence continues to increase in the last years[8,9].

1.2.2 Etiology

Lung cancer has become epidemic over the last century due to the increase of cigarette smoking[5]. The International Agency for Research on Cancer (IARC) listed at least 69 carcinogens in tobacco smoke and identified tobacco-specific N-nitrosamines (TSNAs), which are formed from nicotine, as the most important inducers of lung cancer[10]. These agents are known to bind to DNA and create DNA adducts which, eventually, can lead to permanent mutations[11]. Besides that, TSNAs can activate critical oncogenes, such as KRAS, and damage various tumor suppressor genes loci, for instance, p53-tumor suppressor gene[12,13]. In fact, tobacco was associated with about 80% of the global lung cancer deaths in men and 50% in women[7]. Moreover, it was estimated that 10% of all lung cancers arise in nonsmokers and the remaining 90% arise from long-term smokers[14,15].

Besides tobacco smoking, the exposure to occupational agents, such as radon gas and asbestos, to biomass and wood-smoke, environmental air pollution and infectious agents, constitute also risk factors for developing lung cancer. Likewise, a series of other variables such as genetic factors, gender, race and ethnicity, age and diet are associated with an increase in the susceptibility to develop lung cancer[5].

1.2.3 Lung cancer classification and treatment

Lung tumors are categorized in two main categories according to the histological and genetic features: non-small cell lung cancer (NSCLC) or small cell lung cancer (SCLC). NSCLC, which accounts with approximately 85% of all lung cancer cases, is further classified into three subtypes: adenocarcinoma (AC), squamous-cell carcinoma (SCC) and large cell carcinoma (LCC). AC is the most common type of lung cancer encompassing 40% of all lung cancers and it begins in type II alveolar cells, which secret substances, such as mucus. SCC comprises 25-30% of all lung cancers and it arises from squamous cells that line the inside of lung airways. LCC accounts for 10-15% of lung cancers and appears in any part of the lung[16–18].

The standard treatment options available for NSCLC patients are surgery, chemotherapy and radiotherapy, which are selected according to the staging of the tumor. Patients with lower NSCLC grade stages are subject to surgery to remove the tumor if the tumor is resectable. However, if the tumor is not a candidate for surgical resection, the treatment that is given to the patient is radiotherapy. Patients presenting a higher NSCLC stage, namely, stage IV, that is found in approximately 40% of newly lung cancer patients, are treated with a cytotoxic combination of chemotherapy – cisplatin or carboplatin plus pemetrexed, docetaxel, paclitaxel, gemcitabine, among others[19].

SCLC comprises 15% of all lung cancers and is highly predisposed to early widespread. Thus, all patients, independently of lung cancer stage, are treated with chemotherapy or radiation. However, the overall five-year survival rates round to 6%[19–21].

Nevertheless, over the past two decades, personalized medicine and the search for new specific molecular targets have helped to improve patient's survival and also to reduce disease-related adverse effects. The discovery of recurrent mutations in some tyrosine kinase receptors, such as epithelial growth factor receptor (EGFR) and anaplastic lymphoma kinase (ALK) and some signaling molecules such as MEK1/2 and BRAF, led to the development of effective targeted therapies. For instance, erlotinib and gefitinib were developed to act on EGFR, crizotinib to target ALK, selumitinib and trametinib to inhibit MEK1/2 and vemurafenib to act on BRAF[22]. In the last years, erlotinib, gefitinib, crizotinib and trametinib

were approved by the Food and Drug Administration (FDA) for the treatment of locally and/or metastatic NSCLC[23–25]. In turn, selumitinib and vemurafenib are still under clinical trials for lung cancer[26,27].

Besides targeted therapies, some immunotherapeutic agents and vaccines have been developed to use own body's immune system defense to fight tumor cells. The immunotherapeutic strategies aim to inhibit certain immune checkpoints, which are involved in T-cell activation and proliferation, and in its effector functions that, most times, are repressed by tumor cells[19]. Actually, ipilimumab and tremelimumab were developed to target the T-lymphocyte associated antigen 4 (CTLA-4), which is an inhibitory molecule expressed in tumor cells that inhibits T cell interaction with antigen-presenting dendritic cells and consequently, its activation[22,28]. In addition, the monoclonal antibodies nivolumab and pembrolizumab as well as atezolizumab, durvalumab and avelumab were found to inhibit the interaction between programmed cell-death 1 (PD-1) and its ligand PDL-1, which is known to inhibit T cell survival, proliferation and immune function[22,29]. Both CTLA-4 inhibitors mentioned above and the PD-1/PDL-1 inhibitors atezolizumab, durvalumab and avelumab are undergoing clinical trials whereas nivolumab and pembrolizumab were already approved by FDA for advanced NSCLC treatment[30–36]. Regarding vaccine therapies, some tumor cell or antigen-based vaccines were developed to stimulate immune system to combat tumor cells, such as belagenpumatucel-L (Lucanix®), MAGE-A3, liposomal BLP-25, among others. These vaccines are in clinical trials for lung cancer, including some in phase III[22,28].

The study of genetic mutations and possible new biomarkers allowed the development of several targeted therapies and immunotherapies resulting in significant advances in lung cancer treatment. Nonetheless, this type of cancer remains the first cause of death worldwide. Thus, the search for new targets and consequently, the development of new treatments is in constant progress.

1.3 Hallmarks of cancer

The rationalization of the mechanistic framework of neoplastic diseases may help to understand the organizing principle of cancer cells and thus, develop more effective therapies.

Cancer is a heterogeneous and complex disease which is orchestrated by several distinct cell types, including normal and tumor cells, that actively participate in the tumorigenesis and in the development of a repertoire of biological capabilities that allows tumor cells to survive, proliferate and disseminate. Among these are sustained proliferative signaling, inactivation of growth suppressors, replicative immortality capability, resistance to cell death, angiogenesis induction, activation of invasion and

metastasis, avoidance of immune destruction, genome instability and mutation, tumor-promoting inflammation and deregulation of cellular energetics (Figure 1.2)[37].

Figure 1.2. The ten hallmarks of cancer proposed by Hanahan and Weinberg in 2011. The hallmarks of cancer comprise a number of capabilities involved in the multistep tumorigenesis process that allows tumor cells to survive, proliferate and invade. Adapted from Hanahan and Weinberg, 2011[37].

1.3.1 Cancer metabolism

During the last decades, it has become clear that tumorigenesis as a cell-autologous process based solely on genetic mutations, is not sufficient for tumor growth and metastasis. Indeed, cancer metabolism emerged as an area of research on cancer biology that has increasingly gained attention. This field allowed to understand the processes involved in malignancy transformation and also identified suitable therapeutic targets that are altered in cancer cells[38].

In fact, by the 1920s, Otto Warburg, a German scientist, reported some abnormalities in cancer metabolism[39]. Until then, it was known that in the presence of oxygen, cells convert glucose to pyruvate, which enters into the mitochondria for the oxidative phosphorylation (OXPHOS), whereas under hypoxic conditions, pyruvate is converted into lactate. Interestingly, Warburg found that ascites cancer cells constitutively uptake glucose, being a significant portion converted to lactate, regardless of oxygen availability (Figure 1.3). This metabolic reprogramming was then termed as Warburg effect or aerobic glycolysis[39,40].

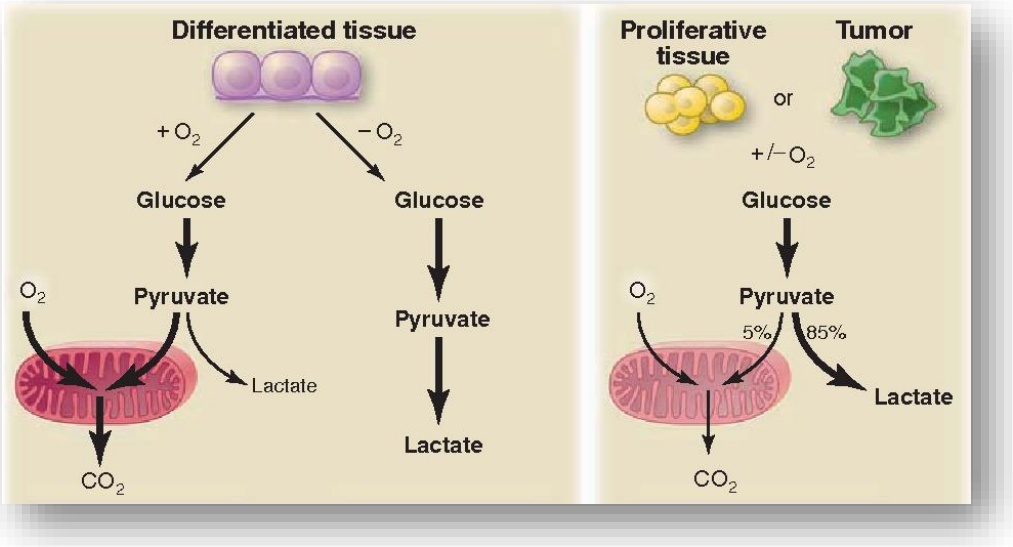

Figure 1.3. Schematic representation of Warburg effect or aerobic glycolysis. In the presence of oxygen, normal cells metabolize glucose to pyruvate, which is oxidized in the mitochondria through oxidative phosphorylation (OXPHOS). When oxygen levels are limited, pyruvate is converted to lactate. Warburg observed that cancer cells produce lactate from pyruvate, regardless of oxygen levels. Adapted from Vander Heiden et al., 2009[40].

Thenceforward, this addictive glycolytic phenotype started to become a distinctive metabolic characteristic of many types of cancer, and subsequently, it was introduced as a new hallmark of cancer in 2011[37].

As first sight, Warburg effect does not appear to be energetically compensatory for cancer cells since glycolysis coupled with OXPHOS generates a substantially greater amount of ATP. However, ATP synthesis through the aerobic glycolysis is 10-100 times faster, supplying the metabolic demands of proliferating cells[41]. In addition, fermentative glycolysis generates metabolites with reducing power, such as NADH, and carbon skeletons for the anabolic pathways. For example, glucose-6-phosphate, a side product of glycolysis, can be deviated to the pentose phosphate pathway, that ultimately, produces ribose-5-phosphate and NAPDH for nucleic acids synthesis. Glyceraldehyde-3-phosphate, another molecule produced during glucose metabolism, can be used for lipid synthesis. Moreover, amino-acids such as serine and glycine, required for protein synthesis, can be produced from 3-phosphoglycerate, a pyruvate precursor (Figure 1.4)[42].

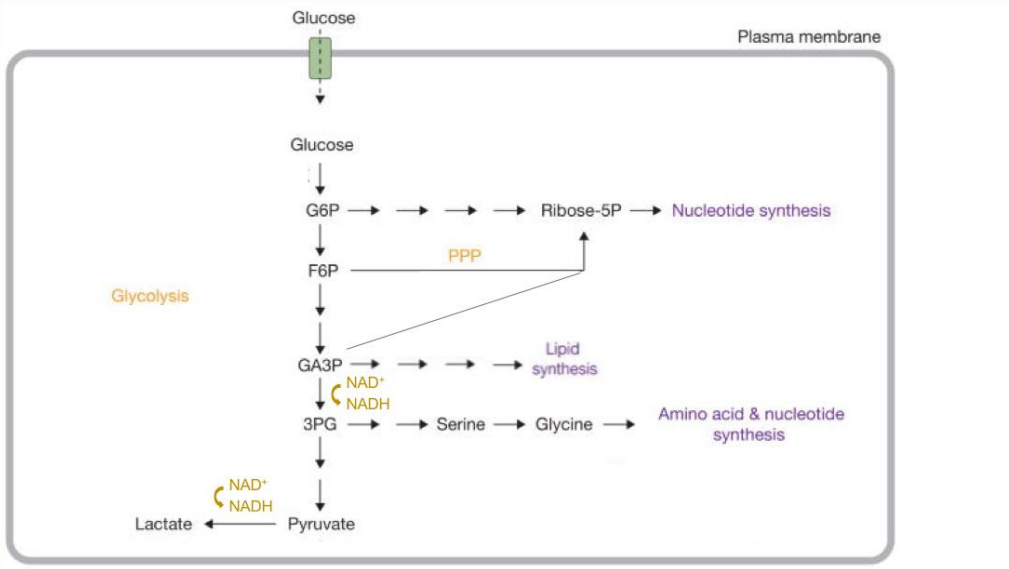

Figure 1.4. Several metabolic intermediates from glycolysis are deviated to the anabolic pathways. Glycolysis provides metabolites with reducing power and carbon sources for the anabolic processes that support cancer cell proliferation. The excess of carbon skeletons is redirected to *de novo* generation of nucleotides and to lipids and protein synthesis (3PG: 3-phosphoglycerate; F6P: fructose-6-phosphate; G6P: glucose-6-phosphate; GA3P: glyceraldehyde-3-phosphate; PPP: pentose phosphate pathway; Ribose-5P: ribose-5-phosphate). Adapted from Vander Boroughs and DeBerardinis, 2015[42].

Beyond the cell-intrinsic functions described above, the Warburg effect was demonstrated to be tightly link with the tumor microenvironment. The upregulation of glycolysis leads to an increase in the intracellular acid lactic content and consequently, the intracellular pH. In order to maintain pH homeostasis and to avoid glycolysis inhibition due to a negative feedback mechanism, cells symport lactate and H^+ ions to the extracellular milieu, leading to an acidification of the tumor microenvironment. Low levels of extracellular pH lead to H^+ diffusion, according to concentration gradients, from tumor cells to the surrounding stroma, a phenomenon that is harmful to normal cells[43–45]. This acidification of tumor microenvironment also protects cancer cells to cell death through the activation of intracellular pathways, such as extracellular-signal related kinase 1/2 (ERK1/2) pathway, which is involved in cell proliferation, differentiation and survival[46].

Moreover, several studies reported that lactate contributes to the modulation of the oncogenic process. This monocarboxylic acid was recognized as a angiogenic inducer since it stimulates the production of vascular epithelial growth factor (VEGF) and its receptor by tumor and endothelial cells, respectively[47,48]. It is also able to induce cell migration by stimulating endothelial cells to produce interleukin-8[49], and to promote tissue remodeling and cell invasion by proteinase induction[50]. Lactate plays also an important role in the escape of tumor cells to the immune system surveillance by decreasing the cytotoxic activity of T-lymphocytes and natural killer cells, reducing dendritic cells maturation and promoting M2-like polarization of tumor-associated macrophages[51].

In this regard, lactate was identified as a key molecule for the tumorigenesis process and its high levels were associated with drug-resistance.

1.4 Monocarboxylate transporters

For many years, it was thought that lactate and other monocarboxylic acids across cellular membranes by non-ionic diffusion of the free acid. However, studies on human red blood cells established the presence of specific carriers in the plasma membrane, being later named as monocarboxylate transporters (MCT)[52,53].

1.4.1 MCTs role, expression and regulation

Monocarboxylate transporters are a family presently composed by 14 members that are encoded by the *Solute Carrier family 16A* (SLC16A) gene[54]. All family members present a similar topology that consists in 12 transmembrane (TM) α-helices domains with intracellular N- and C-termini and a large loop between TM6 and 7 (Figure 1.5)[55].

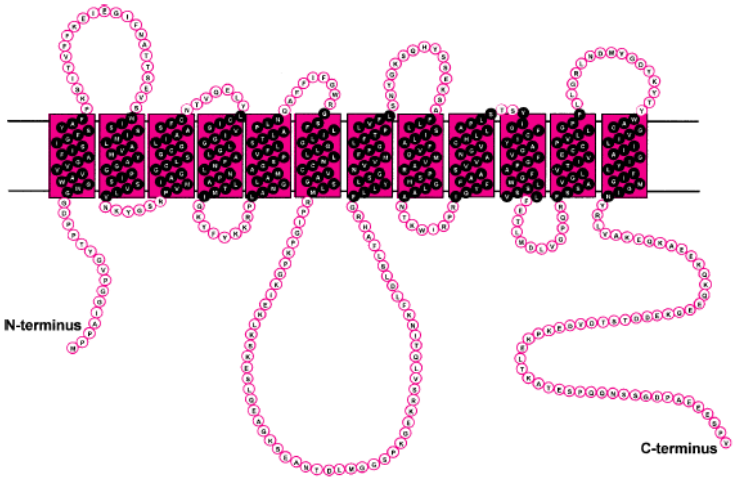

Figure 1.5. Protein diagram of monocarboxylate transporters family proposed by Halestrap and Price. MCTs present 12 transmembrane domains with the N- and C-termini located within the cytoplasm. The sequence shown is from MCT1. Image acquired from Halestrap and Price, 1999[55].

Differences in amino-acids sequences reflected evolutionary divergences related to MCTs functional role[56]. In particular, the first four isoforms (*slc16a1*/MCT1, *slc16a7*/MCT2, *slc16a8*/MCT3 and *slc16a3*/MCT4) were functionally validated to mediate the proton-linked plasma membrane transport of monocarboxylates such as lactate, pyruvate and ketone bodies[57].

MCT1-4 display distinct affinities for monocarboxylic acids that are correlated with the expression patterns of these transporters within the tissues[51]. In general, these four isoforms demonstrate to have a broad specificity for short-chain monocarboxylates, such as L-lactate, pyruvate, D-β-hydroxybutyrate and acetoacetate. However, given their physiological expression, MCT2 exhibits the highest affinities for monocarboxylates, followed by MCT1 and lastly MCT4 (Table 1.1)[54].

Table 1.1. K_M (mM) values of mammalian MCTs isoforms for several metabolic substrates. Adapted from Pinheiro et al., 2012[56].

	MCT1	MCT2	MCT4
L-Lactate	$2.2^{(r)}$–$4.5^{(m*)}$	$0.7^{(r)}$	$28.0^{(h)}$–$34.0^{(r)}$
D-Lactate	$51.0^{(r)}$	–	$519.0^{(h)}$
Pyruvate	$0.6^{(r)}$–$1.0^{(r)}$	$0.08^{(r)}$	$153.0^{(h)}$
L-β-hydroxybutyrate	$8.1^{(r)}$–$11.4^{(m*)}$	n.d.	$824.0^{(h)}$
D-β-hydroxybutyrate	$8.1^{(r)}$–$10.1^{(m*)}$	$1.2^{(r)}$	$130.0^{(h)}$
Butyrate	$9.1^{(h*)}$	n.d.	n.d.
Acetoacetate	$5.5^{(r)}$	$0.8^{(r)}$	n.d.
Benzoate	$1.1^{(h)}$	n.d.	n.d.
Propionate	$1.5^{(r)}$	n.d.	n.d.
Acetate	$3.7^{(m*)}$	n.d.	n.d.

(*n.d.* not determined) (h) – human; (m) – mouse; (r) – rat; (*)- tumor cells

In this regard, MCT1 expression was identified in almost all tissues and has been associated with the uptake or extrusion of lactate and other monocarboxylates through the plasma membrane. Actually, MCT1 was associated with the import of lactate into liver parenchymal cells and kidney tubule cells for the gluconeogenesis pathway, and ketone bodies or lactate into myocytes for OXPHOS. In both muscle and brain, it was described that MCT1 cooperates with other isoforms (*e.g.* MCT2) for the influx or efflux of lactic acid. MCT2 expression is confined to those tissues that take up large quantities of lactate, for example, spleen, heart, kidney and skeletal muscle. Like MCT1, MCT2 is also responsible for the uptake of ketone bodies for OXPHOS. MCT3 has a limited expression in humans, being linked with the efflux of lactate in the retinal pigment epithelium and choroid plexus epithelia. Of note, the transport kinetics of chick MCT3 in a genetically modified yeast revealed a K_m for L-lactate of about 6mM[58]. MCT4 was proposed to have an important role in the export of lactate in tissues with high glycolytic activity related with hypoxic energy production, such as skeletal muscle fibers, astrocytes, white blood cells, chondrocytes, testicle, lung and placenta (Figure 1.6) [58–60].

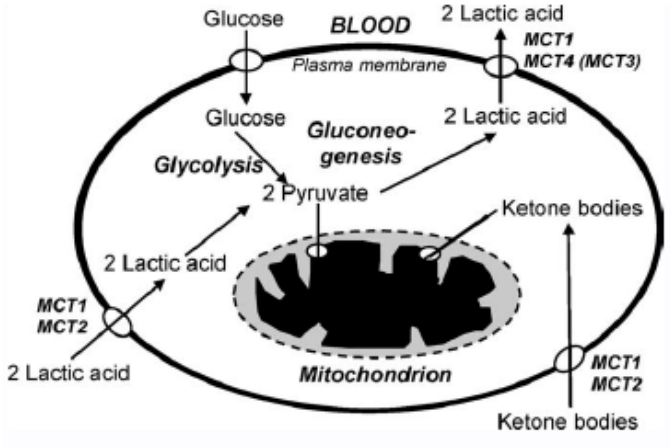

Figure 1.6. MCTs role in cellular metabolism. MCT1 and MCT2 are associated with the influx of lactate and ketones bodies into the cell. MCT3 and MCT4 are known to mediate the efflux of acid lactic, however, MCT1 could also perform this function, depending on MCTs tissue expression. Image acquired from Halestrap, 2012[60].

The differences in MCT expression that are observed between tissues are strictly regulated by a diversity of cellular mechanisms. Although little information is available for MCT2 and MCT3 regulation, many studies emphasize several transcriptional and post-transcriptional regulatory mechanisms for MCT1 and MCT4 expression.

MCT1 has potential binding sites in its promoter for a variety of transcriptional factors, such as c-myc and cAMP-response element-binding protein (CREB)[61,62] whereas MCT4 promoter has two hypoxia response elements for the hypoxia inducible factor 1-α (HIF1-α)[63]. There is also a strong association between the tumor suppressor gene p53[64] and MCT1 up-regulation, as opposed to pro-inflammatory cytokines, such as interferon-γ (IFN-γ) and tumor necrosis factor-α (TNF-α), that are known to decrease its expression[65]. Furthermore, MCT1 and MCT4 overexpression is linked to intense exercise. Over aerobic exercise, large amounts of Ca^{2+} and AMP are produced, that mediate the activation of AMP-activated protein kinase (AMPK) and calcineurin, that ultimately lead to an increase in both MCT isoforms expression[51].

The functional expression of MCTs is regulated by glycosylated accessory proteins that are involved in their trafficking and anchoring at the plasma membrane, allowing their normal activity. MCT1, MCT3 and MCT4 are co-expressed with the cluster of differentiation 147 (CD147) at plasma membrane, whereas MCT2 requires another auxiliary protein named embigin[66].

1.4.2 MCT1/4 as lactate transporters in cancer cells

Of the MCT family, MCT1 and MCT4 isoforms are strongly associated with the hyperglycolytic phenotype of cancer cells[56]. As mentioned before, cancer cells have a heavy demand for glucose[43]. In order to sustain their typical metabolic profile, tumor cells must export lactate derived from the glucose metabolism[46]. Lactic acid is mainly exported by MCT1 and MCT4 isoforms, in order to avoid lactic acidosis and to maintain the glycolytic rates of cancer cells[44]. Indeed, both MCT isoforms have been consistently described as proteins that are upregulated in several solid human tumors, such as colon, glioblastoma, breast, prostate, stomach, and others (reviewed in[56]). In the specific case of lung cancer, our group has previously demonstrated that both isoforms and their chaperone CD147 are overexpressed in lung tumors compared to normal tissues. Particularly, in NSCLC, the squamous cell carcinoma cell type presented higher levels of these proteins in comparison to the adenocarcinoma cases[67].

Taking into consideration MCT1 and MCT4 overexpression in cancer cells and its crucial role in the maintenance of glycolytic rates, the disruption of lactate extrusion showed to be a promising approach for antineoplastic therapeutic targeting. In fact, some reports demonstrated that MCT1/4 inhibition decreased the glycolytic flux and increased the intracellular pH. Subsequently, it leads to cell death *in vitro* and, more importantly, retarded tumor growth *in vivo*[48,68–70].

1.4.3 Role of MCT1/4 in lactate shuttle

The distribution patterns of these two MCTs differ between tumor types and also within the tumor. Some reports associated MCT1 expression with well-oxygenated regions of the tumor tissue whereas MCT4 was reported to be highly express in hypoxic regions. These findings support the notion that within the tumor, there is a metabolic cooperation between cancer cells. Thus, hypoxic cancer cells release lactate through MCT4 to the extracellular medium which is taken up by MCT1 and re-used by oxygenated cancer cells (Figure 1.7)[71].

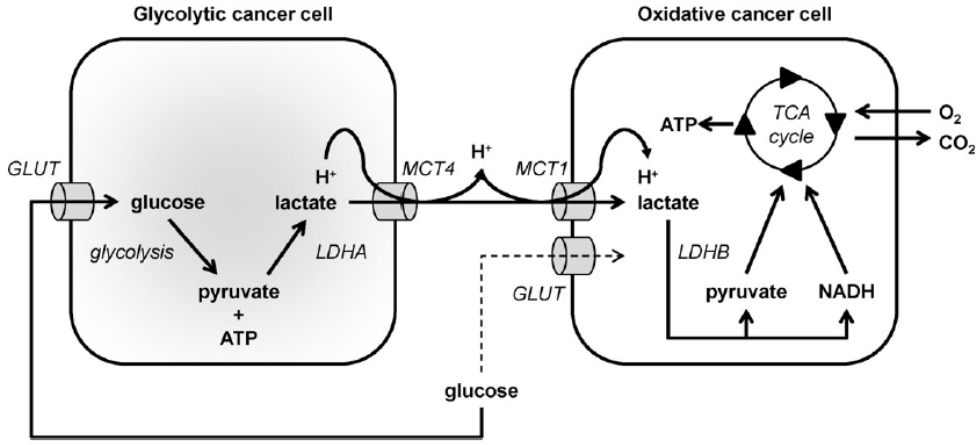

Figure 1.7. Metabolic symbiosis based on lactate shuttle between glycolytic and oxidative cancer cells. Glycolytic cancer cells export lactate through MCT4, which is taken up by MCT1 in oxidative cancer cells. Image acquired from Escuredo et al., 2016[72].

Furthermore, oxidative cancer cells induce an oxidative stress in stroma cells which triggers the expression of MCT4, the glycolytic metabolism and consequently, lactate export. Hence, oxidative cancer cells import lactate via MCT1 (Figure 1.8)[72].

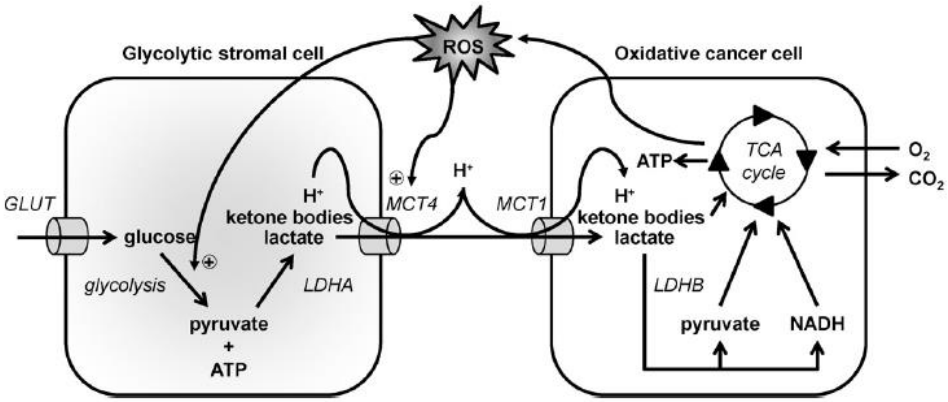

Figure 1.8. Metabolic symbiosis based on lactate shuttle between glycolytic stroma cells and oxidative cancer cells. Glycolytic stroma cells export lactate through MCT4, which is imported by MCT1 in oxidative cancer cells. Image acquired from Escuredo et al., 2016[72].

In the whole, MCT1 and 4 showed to be important carriers involved in lactate shuttle between cancer cells and in the metabolic symbiosis between cancer and stroma cells.

1.4.4 MCT1 and MCT4 inhibition

Owing to the importance of MCT1/4 in the above-mentioned tumor-related biological events, these lactate transporters are considered attractive targets for cancer therapy.

The classical MCT inhibitors comprise fourth main categories: aromatic monocarboxylates (*e.g.* α-cyano-4-hydroxycinnamate (CHC) and phenylpyruvate); amphiphilic compounds including bioflavonoids (*e.g.* quercetin and phloretin); stilbene dissulphonates (*e.g.* 4,4-Odiisothiocyanostilbene-2,20-disulphonate (DIDS) and 4,4-O-dibenzamidostilbene-2,2O-disulphonate (DBDS)) and organomercurial compounds (*e.g. p*-chlomercuribenzene sulfonate (pCMBS))[55]. Although these compounds were reported as having anti-cancer effects, none of them exhibits MCT specificity[73]. Meanwhile, a new class of MCTs inhibitors with high affinity and specificity for these monocarboxylate carriers was developed by AstraZeneca, for instance, AR-C155858, an MCT1/2 inhibitor and its derivative AZD3965, which inhibits MCT1, and AZ93, which acts on MCT4[51]. In particular, the AZD3965 inhibitor is undergoing phase I evaluation after having verified, in preclinical models, that it constrains cancer cell growth. For instance, Polanski and its collaborators demonstrated that AZD3965 was able to increase the intra-tumor lactate and reduce tumor growth *in vivo*. However, Plummer et al. recently reported a little toxicity in the eye and heart in patients treated with this MCT1 inhibitor[74,75].

These compounds showed to be potent MCT inhibitors, however, detailed information about possible side effects is lacking. Besides that, an inherent problem of targeting one isoform is the compensation with another monocarboxylate transporter. In fact, it was reported that MCT1 inhibition led to an increase in MCT4 expression[76], which allowed tumor cells to become resistant to MCT1 inhibitors[68]. Additionally, MCT4 knockdown caused sensitization to MCT1 inhibitors[74]. Therefore, new approaches have to be developed to overcome these issues.

CD147 is known to regulate MCT1/4 activity in human tissues and targeting this auxiliary protein seems to be a rational therapeutic approach against human cancers. In this context, the disruption of CD147 is expected to impair MCT1/4 activity, decrease lactate export and compromise glycolytic flux and cancer cell viability. Indeed, our laboratory group demonstrated that the disruption of CD147 in lung cancer cell lines by Zinc-Finger Nuclease decreased MCT1 and MCT4 expression and activity[67]. Floch et al. showed that CD147 silencing resulted in a down-regulation of both isoforms in colon adenocarcinoma cell lines[68]. A recent report in pancreatic cancer revealed both MCT1 and MCT4 downregulation in CD147-depleted cells[77].

1.5 Cluster of differentiation 147

1.5.1 General features of CD147

Cluster of differentiation 147 also known as basigin (BSG) or extracellular matrix metalloproteinase inducer (EMMPRIN) is a type I transmembrane glycoprotein of immunoglobulin (Ig) superfamily that was discovered in 1982 by Bisway and its collaborators[78,79]. In humans, CD147 is encoded by the *BSG* gene which is located in the chromosome 19 at p13.3[80]. Due to alternative promoters and variations in splicing, *BSG* gene can give rise to four variants: CD147/Bsg-1, which has an additional retina-specific extracellular domain; CD147/Bsg-2, that contains two Ig-like domains; and CD147/Bsg-3 and 4, that have a single extracellular domain (Figure 1.9)[81–83].

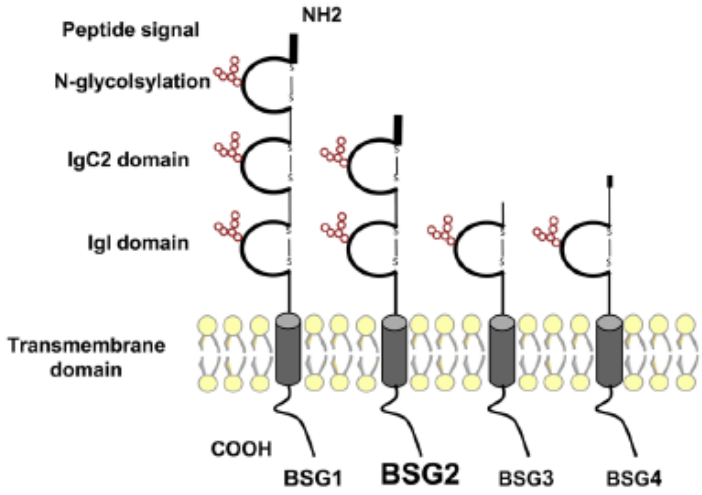

Figure 1.9. Structures of CD147 variants. CD147/Bsg is composed by extracellular immunoglobulin (Ig) domains harboring glycosylation sites (identified as red circles), a single transmembrane spanning segment and a short intracellular tail. Bsg isoforms raised from alternative transcriptional initiation and variations in splicing. Image acquired from Marchiq et al., 2016[51].

The most prevalent and characterized isoform (*i.e.* CD147/Bsg-2) has an encoding region of 269 amino acids, in which the first 21 residues are responsible for cell signaling events and CD147-cell membrane anchor. The following 186 amino acids constitute the extracellular domain, which contains two Ig-like regions at the N-terminal, and the remaining 21 and 41 residues comprise the transmembrane and cytoplasmic domains, respectively[84].

Interestingly, the highly conserved regions of CD147 protein contain distinctive structural characteristics. Ig-domains harbor three conserved asparagine N-glycosylation sites in the extracellular domain that give rise to different CD147 glycoforms depending on glycosylation level. The low-glycosylated forms appear with a molecular mass of ~32kD whereas the high-glycosylated have a molecular weight

between 45-65kD[85]. Moreover, the transmembrane region has a glutamic acid residue and a leucine-zipper motif that are the typical characteristics of proteins that form multi-complexes and the ones involved in cell signaling[86,87].

1.5.2 CD147 expression and regulation

CD147 is ubiquitously expressed at the plasma membrane[88] or in subcellular vesicles[89] of several cell types including neuronal[90], hematopoietic[91], endothelial[92] and epithelial[93] cells. This glycoprotein can also be found in the extracellular milieu, as a soluble form[94].

CD147 expression is controlled by complex regulatory circuits that act at the transcriptional, translation and cell surface expression levels. Over the years, multiple transcriptional factors were described to bind to its promoter region and cooperate to regulate CD147 transcription, for instance, the specific proteins 1 and 3 (Sp1/3) and c-myc[95,96], the early growth response protein 2 (EGR2)[97], HIF-1α[98] and the epithelial-mesenchymal transition (EMT) associated factors, such as Snail and Slug[99]. Following transcription, some miRNAs, such as let-7[100], *miR-146a*[101], *miR-22*[102] and *miR-492*[103], were found to be able to modulate CD147 message levels. Furthermore, soluble mediators, such as epidermal growth factor (EGF), transforming growth factor β (TGF-β)[99], TNF-α[104], interleukin-18[105], nuclear factor κ-light chain-enhancer of activated B cells (NF-$\kappa\beta$) ligand[106], and some hormones, such as progesterone[107], oestrogen[108] and thyroid-stimulating hormone (TSH)[109], have been shown to regulate CD147 transcription and translation.

CD147 expression and localization can be influenced by self-interactions or by interaction with other proteins. CD147 may regulate itself in an autocrine manner via MT1-MMP-dependent cleavage of surface bound CD147[110,111]. Regarding CD147-interacting partners, monocarboxylate transporters, the best characterized partners of CD147, were tightly associated with its correct plasma membrane expression and localization[112,113]. Furthermore, Annexin 2, a multifunctional protein, was found to regulate the cell trafficking of membrane microvesicles harboring CD147 and CD147 release from cells[114]. Cyclophilins were described as proteins that regulate CD147 protein trafficking and cell surface expression[115]. Additionally, the interaction between caveolin-1 and CD147 at the plasma membrane was reported as a way of regulating CD147-self aggregation[85] (Figure 1.10).

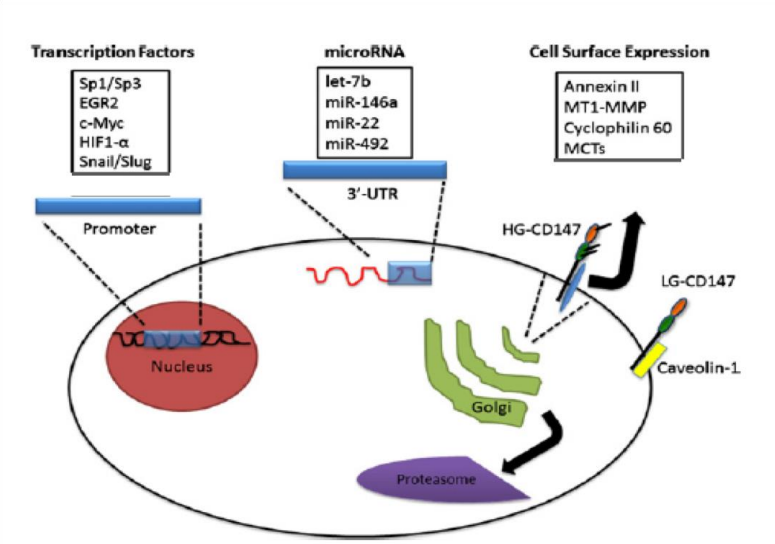

Figure 1.10. Regulatory mediators of CD147 expression. Several transcriptional factors, miRNAs and soluble mediators were described to regulate CD147 expression by transcriptional and translational mechanisms. Additionally, cell surface expression and localization can be influenced by itself interaction or with other proteins. Adapted from Grass et al., 2016[116].

1.5.3 CD147 biological function

CD147 has pleiotropic cellular roles in a diversity of cellular physiological activities. This protein is involved in embryogenesis and spermatogenesis, uterus implantation[117,118] and retinal development[119]. Besides that, CD147 participates in cell adhesion[120], inflammatory responses[121], tissue repair[122] and in sensory and memory events[123]. Nonetheless, CD147 has also been implicated in several pathological events such as rheumatoid arthritis[91], psoriatic skin lesions[124], HIV attachment[125], malaria pathogen invasion[126], Alzheimer pathogenesis[127], among others. Beyond all the healthy and disease events in which CD147 is involved, the best characterized and described function of this protein is in cancer pathology.

1.5.4 Role of CD147 in cancer

CD147, both in a transmembrane or soluble form, has been intensely described as a contribute to the hallmarks of a variety of cancers, including brain, liver, colon, breast and lung (reviewed in[128]). Indeed, it was reported that many tumors overexpressed CD147 and its high expression levels were associated with a poor TMN stage, invasion depth, lymph node metastasis and consequently, poor clinical prognosis and worse survival outcomes[129–133]. The poor outcomes that are observed in cancer patients are mainly due to several cancer events that CD147 is associated, namely, carcinogenesis, metabolic reprogramming and the development of resistance to some chemotherapeutic agents.

Regarding cell membrane-associated CD147, the extracellular portion of the protein mediates the homotypic interactions of CD147 allowing the induction of extracellular matrix metalloproteinases (MMP) via cell-cell interactions. Indeed, CD147 of tumor cells stimulates neighboring fibroblasts to produce MMP-1, MMP-2, MMP-3, MMP-9 and MMP-11 that degrade the extracellular matrix, allowing tumor invasion and metastasis[134]. Besides that, its association with $\alpha 3\beta 1$ and $\alpha 6\beta 1$ integrins, annexin 2 and CD44 glycoprotein is known to mediate tumor invasion and lymph node metastasis[84,89,135]. Furthermore, the extracellular domain of CD147 is known to interact to VEGF receptor in both endothelial and tumor cells, regulating its activation by VEGF and consequently, increasing cell migration and angiogenesis[136]. The transmembrane domain interacts with MCTs, an association that is known to be crucial for the metabolic reprogramming events and the maintenance of the glycolytic phenotype of cancer cells. This interaction occurs between an arginine residue of the TM8 sequence of MCTs and the TM glutamic acid of CD147 (Figure 1.11)[137].

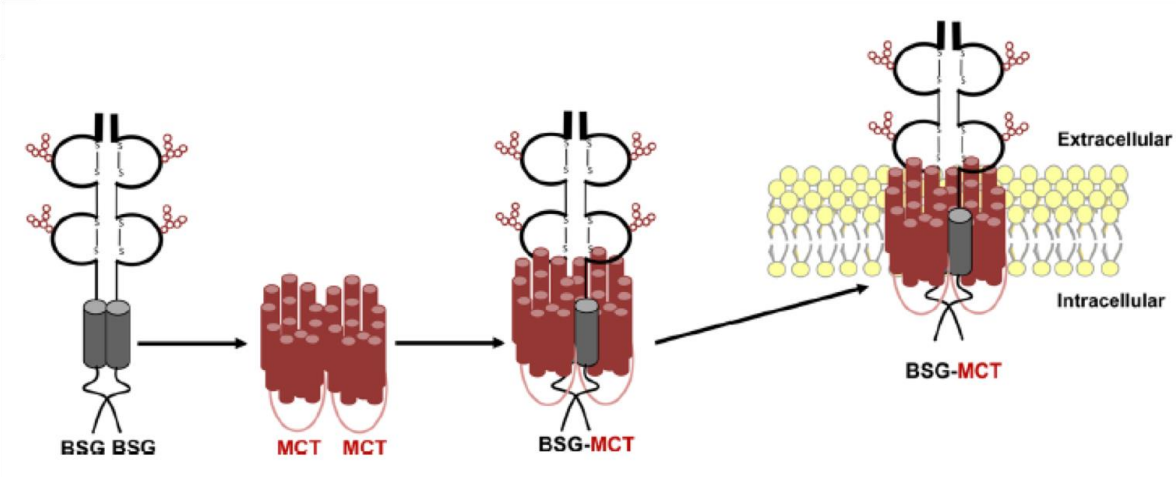

Figure 1.11. Interaction between MCTs and BSG glycoprotein. CD147 dimer binds to two MCT monomers forming a homoligodimer. Image acquired from Marchiq et al., 2016[51].

Concerning soluble CD147, two forms were previously detected in the culture medium of cancer cells and in the serum of patients: the full-length protein or the protein containing only the extracellular portion[138,139].

The full-length protein, which is released by tumor cells via microvesicle shedding, stimulates the production of MMPs by the neighboring fibroblasts and, consequently, enhances the invasiveness capacity of tumor cells[138].

In turn, the protein containing the Ig-like domains, which is generated by proteolytic cleavage of MMPs, interacts with other surface bound CD147 in adjacent and distant stroma cells to further

stimulates the production of MMPs and additional CD147. This positive feedback mechanism is known to contribute to tumor angiogenesis, growth and metastasis[111,139].

1.5.5 CD147 as a therapeutic target

Given the interdependency of MCT1/4 and CD147 for the maintenance of glycolytic flux, and CD147 function in tumorigenesis, CD147 seems to be a promising therapeutic target for cancer malignancies. In fact, some monoclonal antibodies (mAb) against CD147, such as HAb18 mAb; its bivalent fragment HAb18 F(ab')$_2$, also known as Metuximab; the ^{131}I-labeled Metuximab (Licartin) and CNTO3899 were found to inhibit MMP production, cell proliferation and tumor metastasis and growth[140–142]. Recently, a novel small-molecule inhibitor targeting CD147 was found, AC-73. It was reported that it reduced MMP-2 production, decreased hepatocellular carcinoma cells motility and their invasiveness capacity, culminating in a reduction in metastasis formation and tumor growth[143].

Although CD147 neutralization appears to be a good strategy to fight cancer, an inherent problem of targeting cancer cell metabolism is the interconnection between several bioenergetic pathways and their ability to adapt to alterations and switch to a different metabolic phenotype to sustain their cell proliferation and survival[144]. Thus, combined therapies that target more than one bioenergetic markers would be a more clever approach. For instance, our laboratory group demonstrated that CD147$^{-/-}$ lung cancer cells treated with mitochondrial inhibitors, such as phenformin, showed a decrease in cell growth *in vitro* and more importantly, a reduction in tumor growth *in vivo*[67]. Bearing this in mind, the combination of anti-glycolytic and OXPHOS agents seems to be a more effective strategy to eliminate cancer cells.

1.6 Phenformin

Phenethylbiguanide, also known as phenformin, is a biguanide drug that was introduced into the clinics during 1950s for the treatment of diabetes mellitus[145]. However, by 1976, phenformin was withdrawn from the market by FDA because of its association with lactic acidosis[146]. Contrarily to other biguanide drugs, phenformin is more lipophilic and thus, is less dependent on active transport, passing through biological membranes by passive diffusion[147]. This characteristic makes phenformin a more potent biguanide than metformin, another anti-diabetic biguanide[148]. As a positively charged molecule, when phenformin enters into the mitochondria, it accumulates at the mitochondrial matrix because of the mitochondrial membrane potential. Within the mitochondria, phenformin is known to inhibit the complex I (NADH:ubiquinone oxidoreductase) of the respiratory chain leading to an increase of energetic

stress provoked by the absence of ATP in the cell. Under energetic stress, the AMPK pathway is activated through inhibition of the mammalian target of rapamycin (mTOR)[149–151]. Interestingly, the activation of AMPK pathway, the attenuation of ERK signaling and increased oxidative stress were associated with the anti-cancer activity of these biguanides[152].

In 1980, phenformin was, for the first time, associated with an anti-tumorigenic activity[153], and since then, it has been found to have anti-neoplastic effects on several types of cancer, such as pancreatic, liver, breast, lung cancer and others[154–157]. Indeed, phenformin is known to mediate several anti-cancer activities. For instance, it was reported that phenformin is able to inhibit cell proliferation, cell adhesion and invasion, EMT and angiogenesis; induce cell cycle arrest and apoptosis; and more importantly, it decreases tumor metastasis and growth[151,152].

1.7 Nanoparticles as drug carriers

The underlying problems concerning anticancer chemotherapeutics are the poor specificity, high toxicity and the development of drug resistance. In the past few decades, nanocarrier-based platforms have gained increased attention since they showed promising drug delivery features. In fact, they presented advances in the drug pharmacokinetics and biodistribution, and exhibited decreased toxic effects, controlled drug release and sustained delivery of therapeutic agents. Several different types of nanocarriers have been used for cancer therapy, namely liposomes[158].

Liposomes are small artificial vesicles of spherical shape constituted by natural or synthetic phospholipids and cholesterol. These lipid structures are promising anti-tumor drug delivery systems showing numerous advantages over the conventional systems, such as their size and their biodegradable and biocompatible composition[159,160]. Besides that, these nanocarriers present high drug delivery, protect the anti-tumor drug from environmental factors, prevent the early degradation of encapsulated drugs, reduce systemic toxicity and increase concentrations at the target site[161].

Liposomes can have a single (unilamellar vesicles) or multiple bilayered membrane assembly (multilamellar vesicles) of lipids that enclose an aqueous core. They can accommodate water-soluble or lipid-soluble drugs in the aqueous central part or in the lamellae, respectively. Furthermore, they can be covered by polymers, such as polyethylene glycol (PEG) to augment their stability and their half-time in circulation (Figure 1.12)[158,159,161].

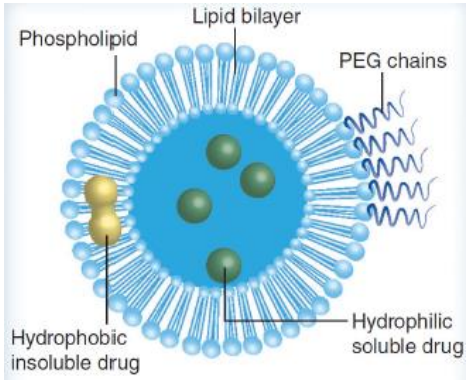

Figure 1.12. Schematic representation of liposome structure. Hydrophilic and hydrophobic drugs can be incorporated in the aqueous part and lamellae of PEGylated liposomes. Adapted from Deshpande et al., 2013[161].

Thus, we aim to enclose phenformin, a potent inhibitor of oxidative phosphorylation, inside liposomes to enhance its efficacy. Furthermore, these liposomes will be coated with antibodies against CD147 in order to specifically guide these nanocarriers to CD147-expressing cancer cells, avoiding a systemic effect of phenformin. With this antibody, we also aim to inhibit glycolysis, preventing the metabolic switch of cancer cells to this pathway.

Chapter 2

OBJECTIVES

2. OBJECTIVES

Metabolic reprogramming renders cancer cells to become addicted to metabolic enzymes or pathways that could be exploited in cancer therapy. In the last decades, this metabolic switch has been substantiated and the development of new therapies targeting cancer metabolism is receiving renewed attention with several drugs entering clinical trials. Nonetheless, the search for suitable targets may be limited by the high metabolic plasticity and the establishment of compensatory routes by tumor cells. Thus, we envision the development of a new therapeutic strategy to attack cancer cells by the combination of anti-glycolytic and anti-OXPHOS agents using targeted drug delivery systems. We foresee that, by targeting and inhibiting the expression of CD147 on the surface of a tumor cell with a CD147-targeted nanoparticle carrying phenformin, we will be able to, on one hand, specifically select/target tumor cells, compromise MCT function and glycolytic rate and, on the other hand, increase the efficacy of phenformin (Figure 2.1). Hence, the general aim of this study is to develop CD147-targeted liposomes carrying phenformin and characterize its efficacy to eliminate cancer cells.

In view of this goal, during this master thesis the following objectives were fulfilled:

I. Characterization of MCT1, MCT4 and CD147 expression and their cellular localization in lung cancer cell lines;

II. Evaluation of the therapeutic effect of phenformin alone on cell growth and metabolism;

III. Determination of anti-CD147 antibody specificity towards CD147-expressing cancer cells and evaluation of several cancer cell features under anti-CD147 antibody treatment;

IV. Assessment of the combination effect of phenformin and anti-CD147 antibody on cell viability, proliferation and metabolism;

V. Evaluation of phenformin-loaded liposomes effect on cell viability, proliferation and metabolism;

VI. Detection of internalized CD147-targeted liposomes carrying phenformin and determination of their efficacy to decrease cell growth.

This research project is focused on a topic that has been shown to have an important implication in the efficacy of current cancer therapies – the Warburg effect. Thus, we expect that this study will unveil new strategies to specifically target tumor metabolism and provide an effective therapy for cancer.

Chapter 3

MATERIALS AND METHODS

3. MATERIALS AND METHODS

3.1 Drugs

The monoclonal Leaf™ Purified Anti-Human CD147 and Leaf™ Purified Mouse IgG1, k Isotype Ctrl antibodies (from now on will be defined as anti-CD147 Ab and isotype ctrl Ab, respectively) were purchased from BioLegend and reconstituted at a stock concentration of 2μg/mL in sterile PBS 1x. Phenformin was purchased from Sigma-Aldrich and a stock concentration of 200mM was prepared by dilution in sterile water. Working concentrations were obtained by diluting these drugs in culture medium. All reagents were stored at -20°C until use. Cell culture medium was used as control (vehicle).

3.2 Large unilamellar vesicles

Large Unilamellar Vesicles (LUVs) were developed in the 3B's facilities according to the thin film hydration method[162] and lipid content was quantified by Bartlett method[163]. Briefly, liposomes were constituted by a single bilayer of phospholipids with long acyl chains (*i.e.* dipalmitoyl phosphatylcholine) and cholesterol, enclosing phenformin in the aqueous core. Cholesterol was labeled with NBD in order to enable the detection of LUVs internalization. The nanoparticles were coated with polymers of poly(ethyleneglycol)(2000)-distearyl phosphatidylethanolamine (DSPE-PEG2000), that were conjugated with the anti-CD147 Ab (Figure 3.1). The development of these nanocarriers was not part of this master thesis.

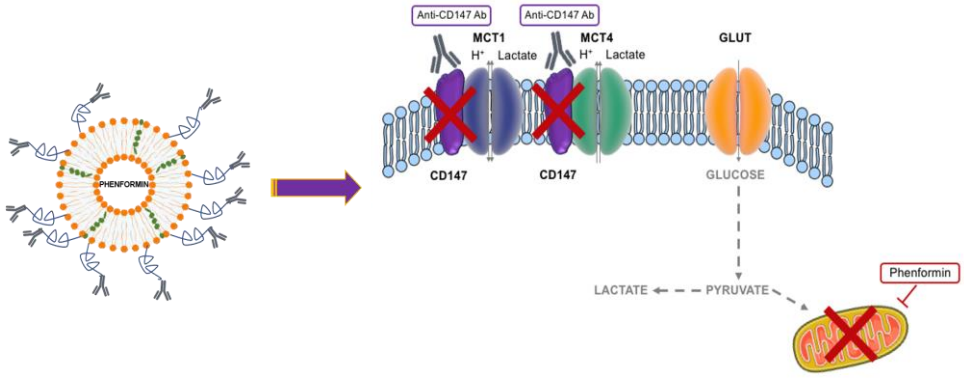

Figure 3.1. Schematic representation of CD147-targeted liposomes carrying phenformin and their intracellular targets. Nanocarriers (represented in the left side) were constituted by a single bilayer of phospholipids and NBD-cholesterol (green), enclosing phenformin in the aqueous core. Liposomes were coated with PEG groups (blue), which were conjugated with the anti-CD147 antibody (grey). The right side of the image represents the function of these nanocarriers. Briefly, phenformin will inhibit OXPHOS and anti-CD147 Ab will compromise CD147-MCT1/4 association and consequently, the glycolytic flux.

3.3 Cell lines and cell culture

The human lung adenocarcinoma A549 and mucoepidermoid pulmonary carcinoma H292 cell lines used in this study were obtained from American Type Culture Collection (ATCC; Manassas, VA, USA). The doubling time of these cell lines is 22h and 48h, respectively. A549 cell line was previously knocked-out for CD147 protein by our laboratory group using Zinc Finger Nucleases[67]. All cell lines were maintained in Dulbecco's Modified Eagle Medium (DMEM) supplemented with 10% of fetal bovine serum (FBS) (both from Biochrom, Merck) and 1% of penicillin (10units/mL) and streptomycin (10μg/mL) (Gibco™, Life Tecnologies Corporation). For normoxic conditions, cells were incubated in a humidified atmosphere of 21% O_2, 5% CO_2 and 74% N_2 at 37°C. For hypoxia induction, cells were placed in an airtight chamber with a hypoxic gas mixture of 1% O_2, 5% CO_2 and 95% N_2 and incubated at 37°C.

3.4 Western blot

Approximately, $1x10^6$ A549 WT, A549 $CD147^{-/-}$ and H292 cells were seeded per standard T25 flask in DMEM 10%FBS and allowed to adhere overnight. Cells were incubated at normoxic or hypoxic conditions for 24 hours. Afterwards, cells were washed in cold PBS, lysed and scraped in lysis buffer (50mM Tris pH 7.6-8.0; 150mM NaCl; 5mM EDTA; 1mM Na_3VO_4; 10mM NaF; 10mM $Na_4P_2O_7$; 1% NP-40) with proteases/phosphatases inhibitors (Roche) and allowed to incubate for 15min for further protein recovery. After a centrifugation of 13000rpm for 15min, total protein was quantified using the Bradford method (Sigma). 30μg of protein was added to an equal volume of Laemmli loading buffer 2x (Bio-rad) and denatured for 10min at 96°C in the ThermoBloc. Proteins were loaded and separated on a standard 10% SDS-PAGE and the polyacrylamide gels were transferred onto nitrocellulose membranes (Amersham Biosciences) using the transferring system Trans-Blot Turbo (Bio-Rad). Blots were blocked in 5% of non-fat milk in TBS 1x 0.1% Tween 20 buffer and incubated overnight with the primary antibodies at 4°C (Table 3.1).

Table 3.1. Details about primary antibodies used in Western blot.

Protein	Company	Reference	Dilution
MCT1	Santa Cruz Biotechnology	sc-365501	1:500
MCT4	Santa Cruz Biotechnology	sc-376465	1:300
CD147	BioLegend	306202	1:500
HIF-1α	BD Biosciences	610958	1:100
β-actin	Santa Cruz Biotechnology	sc-8432	1:500

In the following day, blots were washed three times in TBS 1x 0.1% Tween 20 and incubated with the respective secondary antibodies coupled to horseradish peroxidase for 1h at room temperature (Table 3.2).

Table 3.2. Details about the secondary antibody used in Western blot.

Protein	Company	Reference	Dilution
Goat anti-mouse IgG-HRP	Santa Cruz Biotechnology	sc-2031	1:5000

Blot detection was performed by chemiluminescence using ChemicDocTM XRS+ System (BioRad) after incubation with ECL (SuperSignal West Femto kit, Thermo Scientific).

3.5 Immunofluorescence

Immunofluorescence analysis was used to determine the cellular localization of MCT1/4 and CD147 and to evaluate the specificity of anti-CD147 Ab.

A549 parental and CD147$^{-/-}$ ($8x10^4$/well) and H292 cells ($5x10^4$/well) were seeded on glass coverslips placed into 12-well plates with DMEM 10%FBS and allowed to adhere overnight. Cells were incubated under normoxic or hypoxic conditions for 24h. Afterwards, cells were washed with PBS 1x, fixed and permeabilized with cold methanol during 20min and blocked with 5% bovine serum albumin (BSA) for 30min. Slides were incubated overnight at room temperature with the primary antibodies diluted in 5% BSA (Table 3.3).

Table 3.3. Details about primary antibodies used in immunofluorescence.

Protein	Company	Reference	Dilution
MCT1	Chemicon	ab3538P	1:400 (rabbit)
MCT4	Santa Cruz Biotechnology	sc-376465	1:400 (mouse)
CD147	BioLegend	306202 or 306206	1:400 (mouse)
Isotype Ctrl	BioLegend	400124	1:400 (mouse)

In the following day, cells were washed twice with PBS 1x for 5min and then, the secondary antibodies were applied for 1h at room temperature (Table 3.4).

Table 3.4. Details about secondary antibodies used in immunofluorescence.

Protein	Company	Reference	Dilution
Alexa Fluor 594 goat anti-mouse	Life Technologies	A11032	1:400
Alexa Fluor 568 goat anti-rabbit	Life Technologies	A11011	1:200
Alexa Fluor 488 goat anti-mouse	Life Technologies	A11001	1:400

Slides were mounted using Fluoroshield™ Mounting Media containing 4',6-diamidino-2-phenylindole (DAPI) (Sigma-Aldrich). Images were obtained with a fluorescent microscope (Olympus BX16), using the Cell P software.

3.6 Cell viability assay

The sulforhodamine B (SRB) assay was used for the following experiments:

- To determine the half maximal inhibitory concentration (IC_{50}) of phenformin;
- To evaluate cell viability upon treatment with anti-CD147 antibody alone or in combination with phenformin;
- To assess the efficacy of liposomes carrying phenformin treatment.

Cells were plated at an initial concentration of $8x10^3$ (A549 WT and $CD147^{-/-}$) or $5x10^3$ (H292) per well into 96-well plates and allowed to adhere overnight. Cells were incubated in DMEM 1%FBS with phenformin (0.01-4mM) and anti-CD147/isotype ctrl antibodies (10-1000ng/mL) alone or in combination with phenformin (300ng/mL and 0.5mM, respectively) or with LUVs/LUVs carrying phenformin (0.01-

8mM). After 24h, 48h or 72h, cells were fixed with cold 10% trichloroacetic acid (TCA) for at least 1h at 4°C and stained with Sulforhodamine B (Sigma-Aldrich) for 30min. To remove the excess of dye, cells were washed repeatedly with 1% acetic acid and protein-bound dye was dissolved in 10mM of Tris-Base solution (pH=10.5) for absorbance measurement at 530nm using the Thermo-Scientific Varioskan Flash SkanIt software (Thermo-Scientific). All results were normalized to the respective controls.

3.7 Extracellular lactate measurements

Lactate content in the culture medium was measured to analyze the effect of phenformin, anti-CD147 Ab and of LUVs carrying phenformin.

A549 WT and H292 cells were plated in 48-well plates at a density of $1.2x10^4$ and $1.0x10^4$ cells per well, respectively and allowed to adhere overnight. Cells were incubated with DMEM 10%FBS supplemented with phenformin (0.5mM), anti-CD147/isotype ctrl antibodies (50-300ng/ml) alone or in combination with phenformin (300ng/ml and 0.5mM, respectively) or with LUVs/LUVs carrying phenformin (1-4mM) under normoxic and hypoxic conditions for 24h. Lactate content was analyzed in the cell culture supernatant using a commercial kit (Spinreact), in which 100μL of the commercial reagent are added to 2μL of the sample in 96-well plates. After 10min of reaction, the OD was measured at 490nm in the Varioskan Flash reader using the SkanIt software. Lactate quantification was calculated using a standard curve. Results are expressed as total μg/ total biomass. Total biomass was assessed through SRB assay, as previously described.

3.8 Three-dimensional cell culture

Single cell suspensions of $5x10^3$ A549 WT and H292 cells were seeded per well on agarose-coated 48-well plates. Plates were centrifuged at 1200rpm for 5min and incubated in a 37°C, 5% CO_2 incubator. After five days, spheroids were incubated with phenformin (1-2mM) or LUVs/LUVs carrying phenformin (1mM) diluted in DMEM 10%FBS. Spheroid morphology was observed along time and images were collected using the Olympus IX51 microscope. Tumor spheroid area was determined using the ImageJ software.

3.9 Clonogenicity assay

A549 WT and H292 cells were seeded in 6-well plates in DMEM 10%FBS at a density of 500 cells per well to evaluate colony formation. Cells were then incubated under normoxic or hypoxic conditions with a media containing anti-CD147 or isotype ctrl antibodies (200-300ng/mL), phenformin (10-50µM) alone or in combination with the anti-CD147 Ab (10µM and 300ng/mL, respectively), according to the following diagram (Diagram 1):

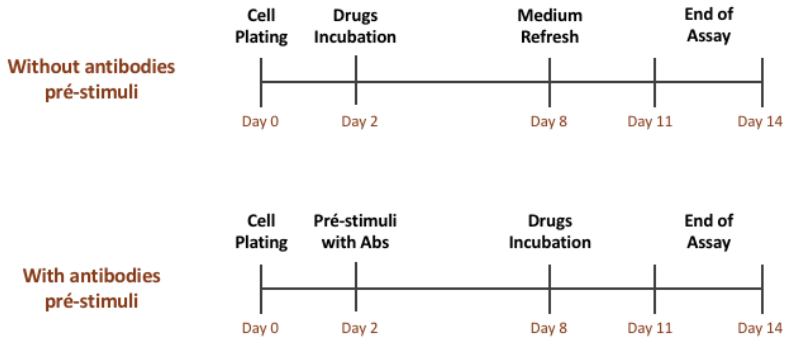

Diagram 1: Chronological representation of the various steps performed in the clonogenicity assay.

At the end of the experiment, cells were washed with PBS 1x and stained with 20% Giemsa (Fluka) in methanol for 45min at room temperature.

3.10 Wound-healing assay

Approximately, $9x10^5$ of A549 WT cells and $8x10^5$ of A549 CD147$^{-/-}$ and H292 cells were plated per well in 6-well plates and cultured to at least 95% confluence. Monolayer cells were scraped with a plastic pipette tip, washed with PBS 1x and incubated under normoxic or hypoxic conditions with 300ng/ml of anti-CD147 or isotype ctrl antibodies diluted in DMEM 10%FBS. Images of wound areas were taken after 5h, 8h, 24h or 48h of incubation using the Olympus IX51 microscope. The migration distance was measured using the *beWound* software (version 1.7, BeSurg)[69]. For each time point, the migration distance, in percentage, was calculated with the following formula (Equation 1):

$$W(\%) = 100 - \frac{W_t \times 100}{W_0}$$

Equation 1: Mathematical formula for wound closure determination. (W= Wound closure; W_t= width of wound closure; W_0= initial width of the wound.

The percentage of wound closure of the treated groups was then normalized for the controls.

3.11 Cell invasion assay

This assay was performed using spheroids as previously described. After 5 days, spheroids were transferred into 96-well plates and incubated with 300ng/ml of anti-CD147 Ab diluted in matrigel. Spheroid morphology was observed along time and images were collected using the Olympus IX51 microscope. The area of spheroids and spheroids invaded area were determined using the ImageJ software.

3.12 Cell proliferation assay

A549 WT and H292 cells were plated in 96-well plates at a density of $8x10^3$ and $5x10^3$ cells per well, respectively, and allowed to adhere overnight. Afterwards, cells were synchronized for 2h in starvation medium and then, incubated with 1-4 mM of LUVs or LUVs carrying phenformin diluted in DMEM 1%FBS. After 24h of treatment, cell proliferation was assessed using the BrdU Cell Proliferation ELISA assay (from Roche) according to the manufacturer's protocol. Briefly, 100µL of BrdU label diluted in DMEM 1%FBS were added to each well and incubated for 4h. Afterwards, cells were fixed, and DNA was denatured with 200µL of FixDenat for 30min. 100µL of Anti-BrdU-POD antibody were added to the cells and incubated for 90min. After washing three times with PBS 1x, cells were incubated with 100µL of tetramethyl-benzidine (TMB) substrate for 5min. The reaction was stopped by adding 25µL of 1M H_2SO_4. Absorbance was measured at 450nm in the Varioskan Flash reader using the SkanIt software.

3.13 Statistical analysis

To evaluate the lactate extrusion upon treatment with phenformin, a paired two-tailed t-test was carried out. For the remaining quantifications of extracellular lactate, an unpaired two-tailed t-test was applied in order to compare the treated groups with the respective controls. Regarding 3D-cell culture growth, cell migration and cell invasion assays, a two-way ANOVA post-hoc Sidak's test was applied and multiple comparisons were performed. To assess the effect of liposomes on cell viability, a one-way ANOVA post-hoc Dunnett's test was used. All analyses were performed in *GraphPad Prism* (GraphPad Prism software, Inc., version 6) and statistically significant differences were considered when *p-values* were lower than 0.05.

Chapter 4

RESULTS

4. RESULTS

4.1 MCT1, MCT4 and CD147 are expressed in lung cancer cells

To study the expression of MCT1, MCT4 and CD147 in lung cancer cells, we first analyzed their protein levels in the adenocarcinoma A549 WT and A549 CD147$^{-/-}$ cells and in the mucoepidermoid pulmonary carcinoma H292 cells by Western blot. The results showed that MCT1, MCT4 and CD147 are expressed in A549 WT and H292 cells, whereas in A549 CD147$^{-/-}$ cells no expression was found. Furthermore, MCT1 and MCT4 expression increased under hypoxic conditions (Figure 4.1A). Next, by immunofluorescence, we evaluated their cellular localization. All proteins are present in the cytoplasm and especially in the plasma membrane of the A549 WT and H292 cells (Figure 4.1B).

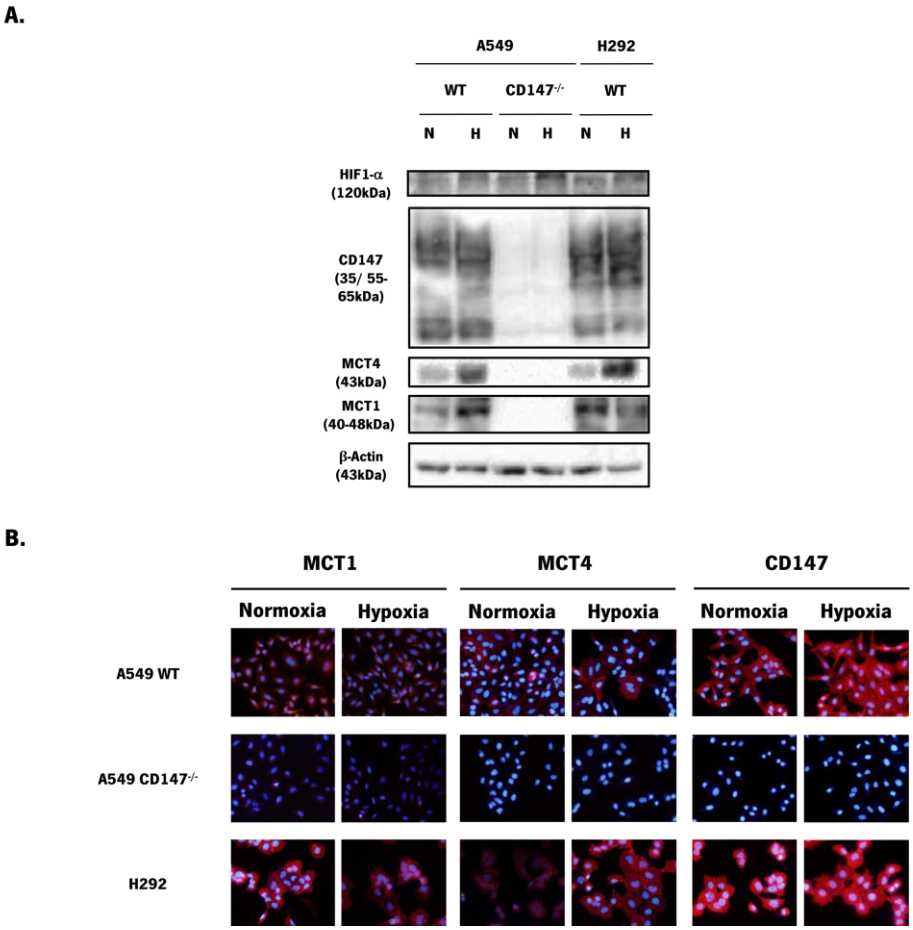

Figure 4.1. Monocarboxylate transporters 1/4 and CD147 are expressed in lung cancer cell lines. (A) Western blot and **(B)** immunofluorescence staining of MCT1, MCT4 and CD147 in A549 WT, A549 CD147$^{-/-}$ and H292 cells exposed to normoxia (N) or hypoxia (H) for 24 hours (n=1). β-actin was used as loading control. Immunofluorescence images were taken at 200x magnification (DAPI (blue) – nuclei; Red – MCT1, MCT4 or CD147).

4.2 Phenformin decreased 2D and 3D-cell growth and increased lactate production

Since we aimed to incorporate phenformin in nanoparticles, we primarily tested the effect of phenformin in NSCLC cells. Phenformin is described to impair mitochondrial respiration by the inhibition of complex I of the respiratory chain. Such OXPHOS impairment leads to an activation of AMPK/mTOR pathway which culminates in a compensatory acceleration of glycolysis, an increase in ROS production and cell death[164]. Bearing this in mind, we evaluated the influence of phenformin in the viability of A549 WT and H292 lung cancer cells by sulphorhodamine B assay. Both cell lines showed sensitivity to phenformin in a dose-dependent manner, with H292 cells being slightly more sensitive than A549 WT (Figure 4.2A). Given the sensitivity of NSCLC cells to phenformin, we further analyzed if phenformin could disrupt OXPHOS and, consequently increase the glycolytic rates and lactate production. Although no significant results were found for 0.5mM of phenformin, it was possible to observe a tendency for phenformin to increase the lactate production, suggesting that phenformin was able to inhibit the complex I of the mitochondria (Figure 4.2B).

Since three-dimensional cell cultures better reflect the *in vivo* microenvironment in terms of nutrient and oxygen gradients and cell-cell interactions than 2D-cell cultures[165], we next investigated the effect of phenformin in 3D-tumor spheroid growth. In accordance to what we observed in Figure 4.2A, phenformin was able to decrease A549 WT and H292-tumor spheroid size (Figure 4.2C). Altogether, these results showed that A549 and H292 cells were sensitive to the anti-cancer effect of phenformin and thus, it is a putative drug to introduce in nanoparticles.

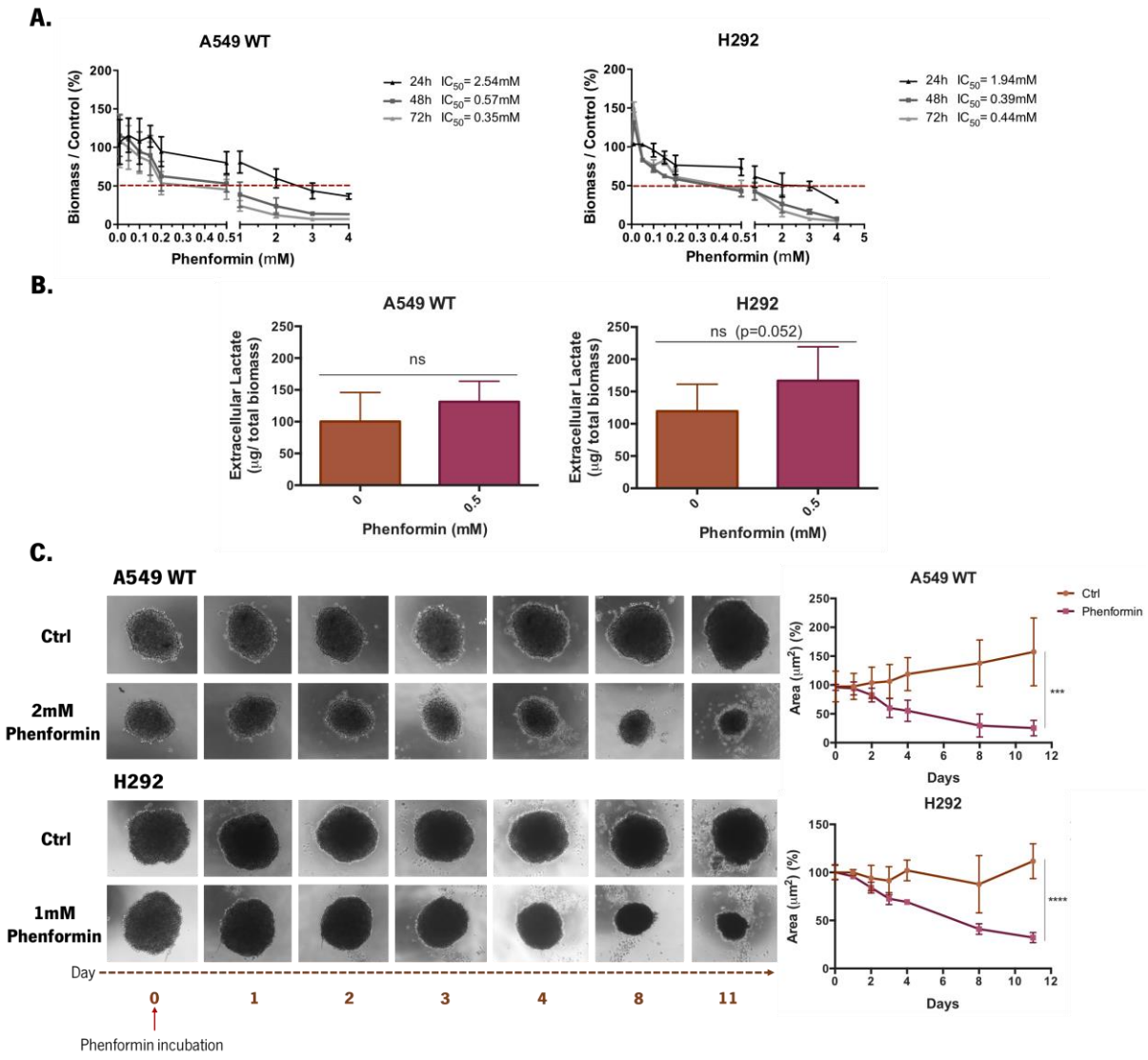

Figure 4.2. Phenformin decreased 2D and 3D-lung cancer cell growth and increased lactate production. (A) A549 WT and H292 cell viability was assessed by sulphorhodamine B (SRB) assay after 24, 48 and 72 hours of incubation with increasing concentrations of phenformin (0.01-4mM; n=5). **(B)** Extracellular lactate was quantified in both cell lines after 24 hours of incubation with 0.5 mM of phenformin using a commercial enzymatic colorimetric kit (n=2). **(C)** A549 WT and H292 3D-spheroids growth was analyzed for 11 days after treatment with 2mM or 1mM of phenformin, respectively (representative images are shown; magnification: 40x; n=2). Results are represented as mean ± standard deviation (ns - not significant; ***p<0.001; ****p<0.0001. Paired two-tailed t-test was applied in the extracellular lactate quantification assay and two-way ANOVA post-hoc Sidak's test in 3D-spheroids growth assay).

4.3 Lung cancer cell viability and CD147 function was not compromised by the anti-CD147 Ab treatment

One of the aims to develop anti-CD147 loaded liposomes is to enhance selective drug delivery to tumor cells and, at the same time, enable the inhibition of the glycolytic pathway. To accomplish this aim, we selected an anti-CD147 antibody, the Leaf™ Purified Anti-Human CD147 antibody from BioLegend

that due to its endotoxin composition is known to target and inhibit CD147 at the surface of a tumor cell. Therefore, it was expected that CD147 inhibition would compromise MCT1/4 activity and lactate extrusion from tumor cells and ultimately, induce cell death, as previously described[166].

In this sense, we started by evaluating the specificity of this particular antibody to CD147 protein. For that purpose, A549 WT and A549 CD147$^{-/-}$ cells were used to evaluate, by immunofluorescence, the expression of CD147 using this specific antibody. The results revealed anti-CD147 Ab was specific for CD147-expressing cells since only A549 WT exhibited its expression in the opposite to A549 CD147$^{-/-}$ cells (Figure 4.3A).

We further selected a range of antibody concentrations that would not compromise cell viability by toxicity. For that purpose, we incubated A549 WT and CD147$^{-/-}$ cells and H292 cells with increasing doses of the respective isotype ctrl Ab, which has the same Ig as the anti-CD147 Ab but with no variable region for CD147. Between 10 and 300ng/ml of antibody, no cytotoxic effects were observed (Figure 4.3B) but, if higher concentrations of antibody were used, cell viability was compromised (Figure 4.4B). Thus, we incubated these lung cancer cells with the anti-CD147 Ab, at non-toxic concentrations, to study its effect on cell viability. As shown in Figure 4.3C, anti-CD147 Ab did not compromise cell viability in all cell lines.

Although no effects on cell viability were found, we next quantified the extracellular lactate levels in antibody-treated NCSLC cells in order to understand if anti-CD147 Ab could compromise lactate transport. We verified that none of the concentrations tested were able to decrease the lactate release from lung cancer cells (Figure 4.4A) Overall, these data demonstrated Leaf™ Purified Anti-Human CD147 antibody was able to specifically target CD147, however it was not able to inhibit its function as MCTs chaperone.

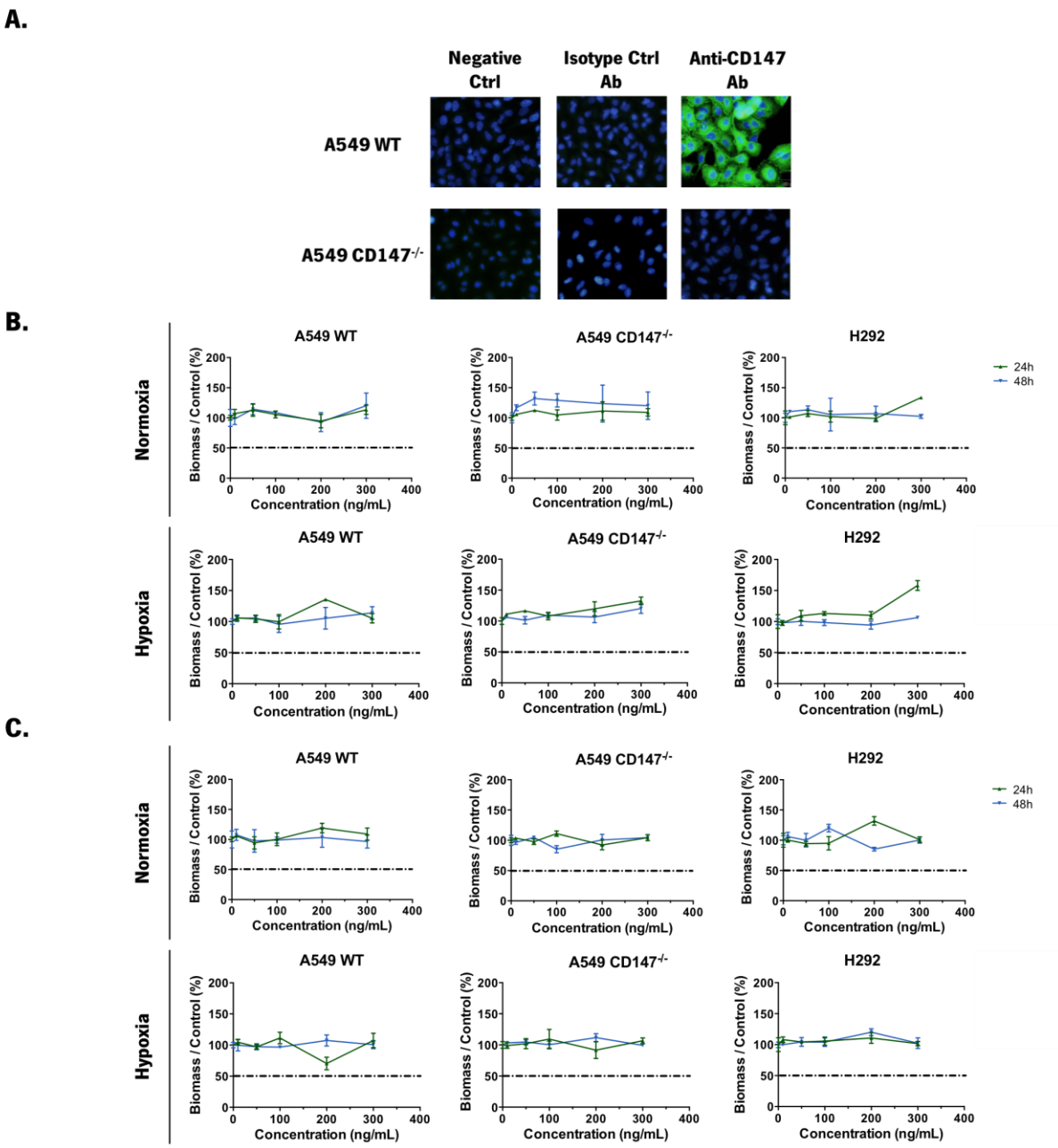

Figure 4.3. Leaf™ Purified Anti-Human CD147 antibody did not compromise NSCLC cell viability. (A) Immunofluorescence analysis of anti-CD147 Ab in A549 WT and A549 CD147$^{-/-}$ cells (n=1). Images were taken at 200x magnification (DAPI (blue) – nuclei; Green – CD147). Increasing concentrations (10-300ng/ml) of isotype ctrl **(B)** or anti-CD147 **(C)** antibodies were given to A549 WT, A549 CD147$^{-/-}$ and H292 cell lines and cell viability was assessed by SRB assay after 24 and 48 hours (a representative experiment of at least 2 independent assays is shown).

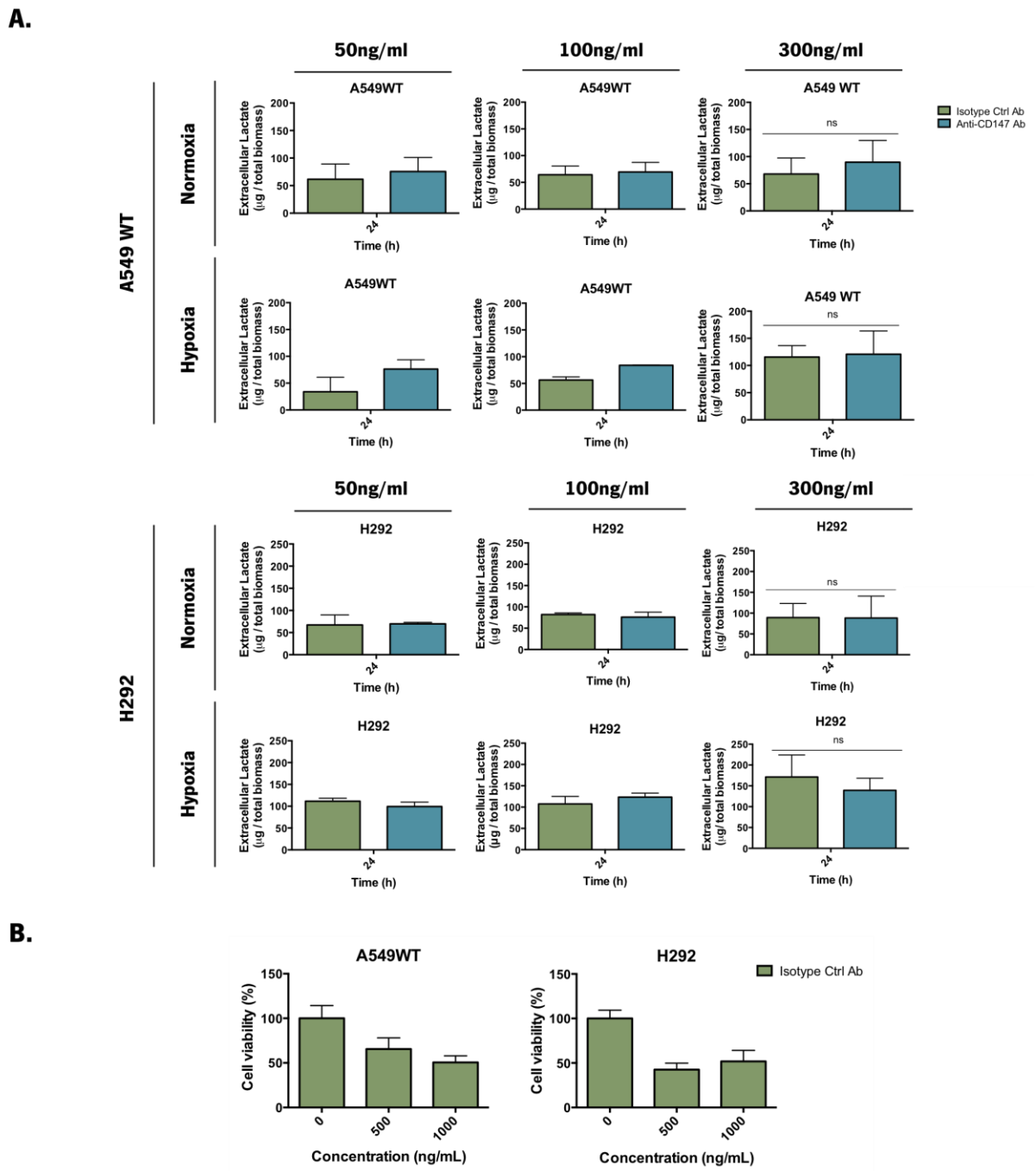

Figure 4.4. Leaf™ Purified Anti-Human CD147 antibody did not impair lactate export in NSCLC cells. (A) Extracellular lactate was quantified in A549 WT and H292 cells after 24 hours of incubation with 50 (n=1), 100 (n=1) or 300ng/ml (n=3) of isotype ctrl and anti-CD147 antibodies under normoxic or hypoxic conditions, using a commercial enzymatic colorimetric kit. Results were normalized for the total biomass, which was assessed by SRB assay. **(B)** A549 WT and H292 cell viability was analyzed by SRB assay, after 24 hours of incubation with 500 or 1000ng/ml of isotype ctrl Ab (n=1) under normoxic conditions. Results are represented as mean ± standard deviation (ns - not significant. Unpaired two-tailed t-test was applied for extracellular lactate quantification assay).

4.4 Anti-CD147 Ab combined with phenformin did not impair cell viability or lactate extrusion

We have previously observed that there was no effect on cell viability (Figure 4.3C) and lactate export (Figure 4.4A) in cells treated with anti-CD147 Ab alone. Since cancer cells are highly plastic cells with the ability to switch their own metabolism, we further investigated if we blocked mitochondrial respiration with phenformin, cells would be more sensitive to the anti-CD147 Ab. For that purpose, we treated A549 WT and H292 cells with the combination of anti-CD147 Ab and phenformin and we evaluated cell viability and lactate production. The decrease on cell viability observed in both cell lines was mainly caused by the phenformin treatment, since no differences were observed on cell viability between phenformin or its combination with the anti-CD147 Ab (Figure 4.5A).

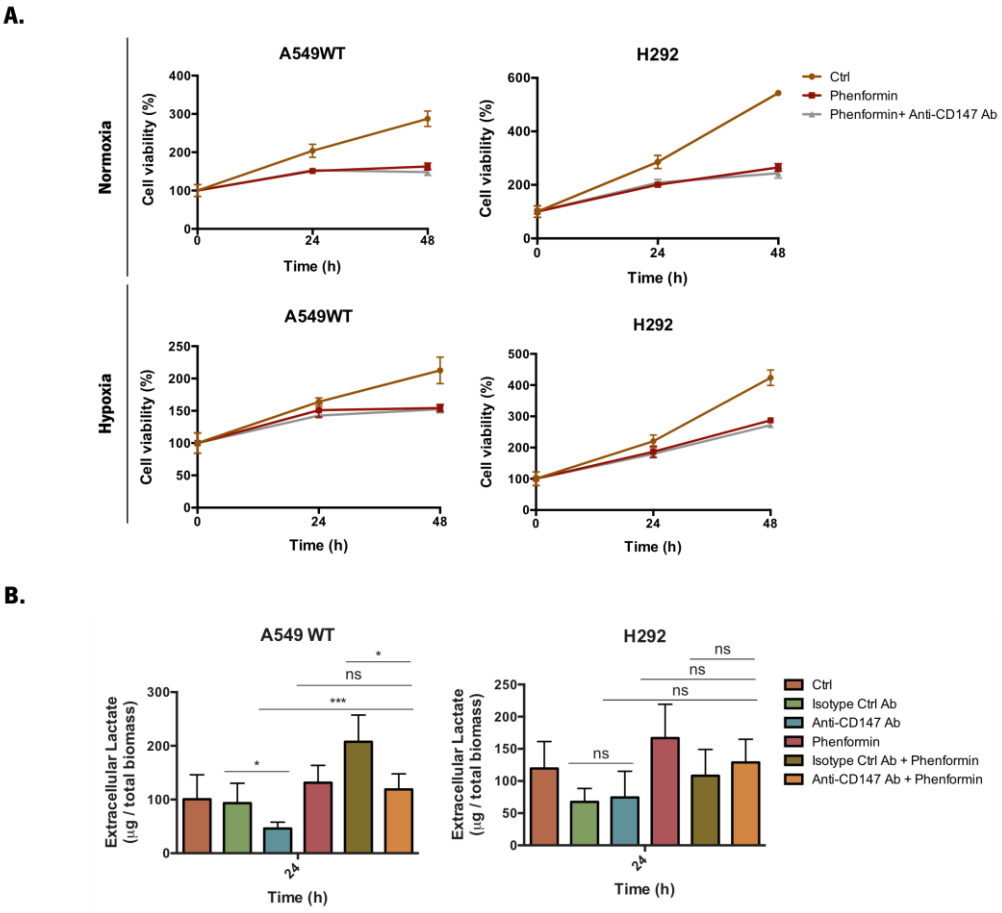

Figure 4.5. The anti-CD147 Ab in combination with phenformin did not compromise cell viability and lactate extrusion. (A) A549 WT and H292 cell viability was assessed by SRB assay after 24 and 48 hours of incubation with 0.5mM of phenformin alone or in combination with 300ng/ml of anti-CD147 Ab under normoxia or hypoxia (n=1). **(B)** Extracellular lactate was quantified after 24 hours of incubation with 300 ng/ml of isotype ctrl or anti-CD147 antibodies, 0.5mM of phenformin or their combinations under normoxic conditions, using a commercial enzymatic colorimetric kit (n=2). Results were normalized for the total biomass, which was assessed by SRB assay. Results are represented as mean ± standard deviation (ns - not significant; *p< 0.05; ***p< 0.001. Unpaired two-tailed t-test was applied to compare extracellular lactate levels in treated and the respective control groups).

Also, when we analyzed the extracellular lactate content no significantly differences were observed between the combination of anti-CD147 Ab and phenformin compared to phenformin alone (Figure 4.5B).

4.5 The anti-CD147 Ab inhibits cell migration and cell invasion

So far, we showed that the anti-CD147 antibody did not compromise CD147 function as a MCT1/4 chaperone, and consequently, no alterations in lactate export were observed. Before being recognized as a chaperone of MCTs, CD147 was described to have an important role in several features of cancer aggressiveness. Its role in important malignant processes such as cell proliferation, migration and invasion is well recognized[84]. Thus, we went to analyze the effect of anti-CD147 Ab on these events.

To evaluate cell proliferation, the clonogenicity assay was carried out and the ability of A549 WT and H292 cells to form colonies under treatment with phenformin, anti-CD147 Ab alone or in combination was evaluated. In accordance with the previous results, phenformin decreased A549 WT and H292 cell proliferation whereas no effects were found for the anti-CD147 Ab (Figure 4.6A). Thus, we thought that if we pre-stimulated cells with the antibody, we would be able to sensitize them to its effect before the treatment with the combination of both drugs. However, the pre-stimulus with the antibody did not impact on clonal growth (Figure 4.6B).

Next, we studied the effect of anti-CD147 Ab on lung cancer cell migration using the wound-healing assay. Some studies associated CD147 inhibition by immunotherapy with a decrease in cell migration, via downregulation of EGFR pathway[167]. Our data showed that in hypoxic conditions, A549 WT and A549 CD147$^{-/-}$ cells migrated less under anti-CD147 Ab treatment when compared to isotype ctrl Ab (Figure 4.7). In general, it was also observed a tendency for cell migration inhibition in all cell lines in the first hours, although not statistically significant.

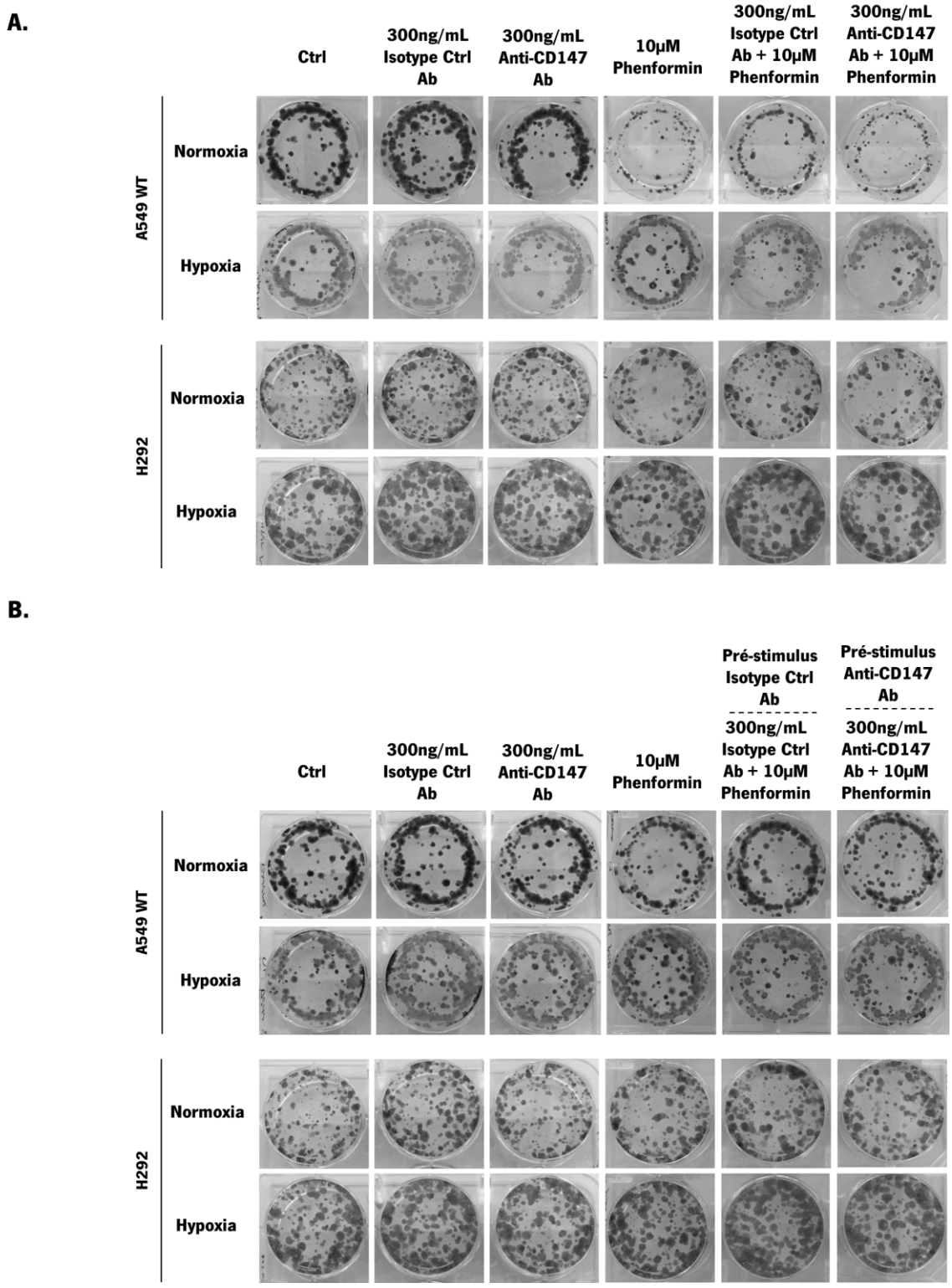

Figure 4.6. The anti-CD147 Ab did not compromise the capacity of NSCLC cells to growth. Clonogenicity assay was carried out in A549 WT and H292 cells treated with 300ng/ml of isotype ctrl or anti-CD147 antibodies, 10µM of phenformin and their combination without **(A)** or with **(B)** a pré-stimulus with 300ng/ml of isotype ctrl or anti-CD147 antibodies under normoxia or hypoxia (representative images from at least 2 independent assays are shown).

Afterwards, we went to explore the impact of anti-CD147 antibody on CD147 activity as an MMP-inducer. Indeed, some monoclonal antibodies against CD147 were described to decrease MMP production and consequently, cell invasion[166]. Thus, to study cell invasion, we generated A549 WT, A549 CD147$^{-/-}$ and H292 3D-cell spheroids and then, we incubated them in matrigel containing the anti-CD147 antibody. The anti-CD147 Ab demonstrated to be able to inhibit the invasiveness capacity of A549 WT cells contrarily to A549 CD147$^{-/-}$ cells. Although no significant results were found for H292 cells, a decrease trend was noted on cell invasion upon anti-CD147 Ab treatment (Figure 4.8).

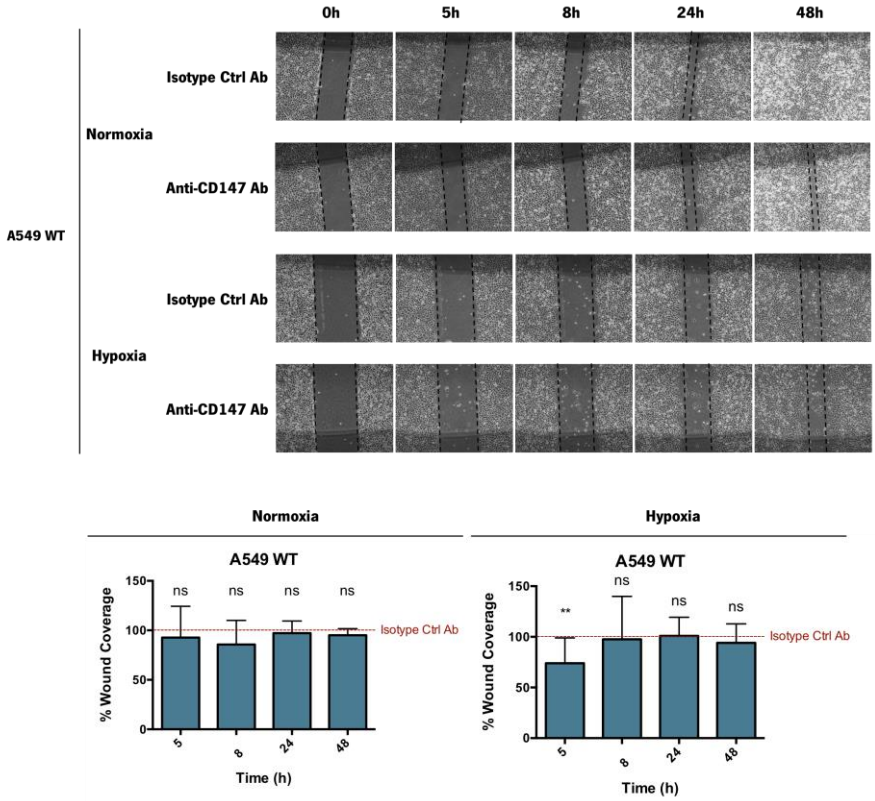

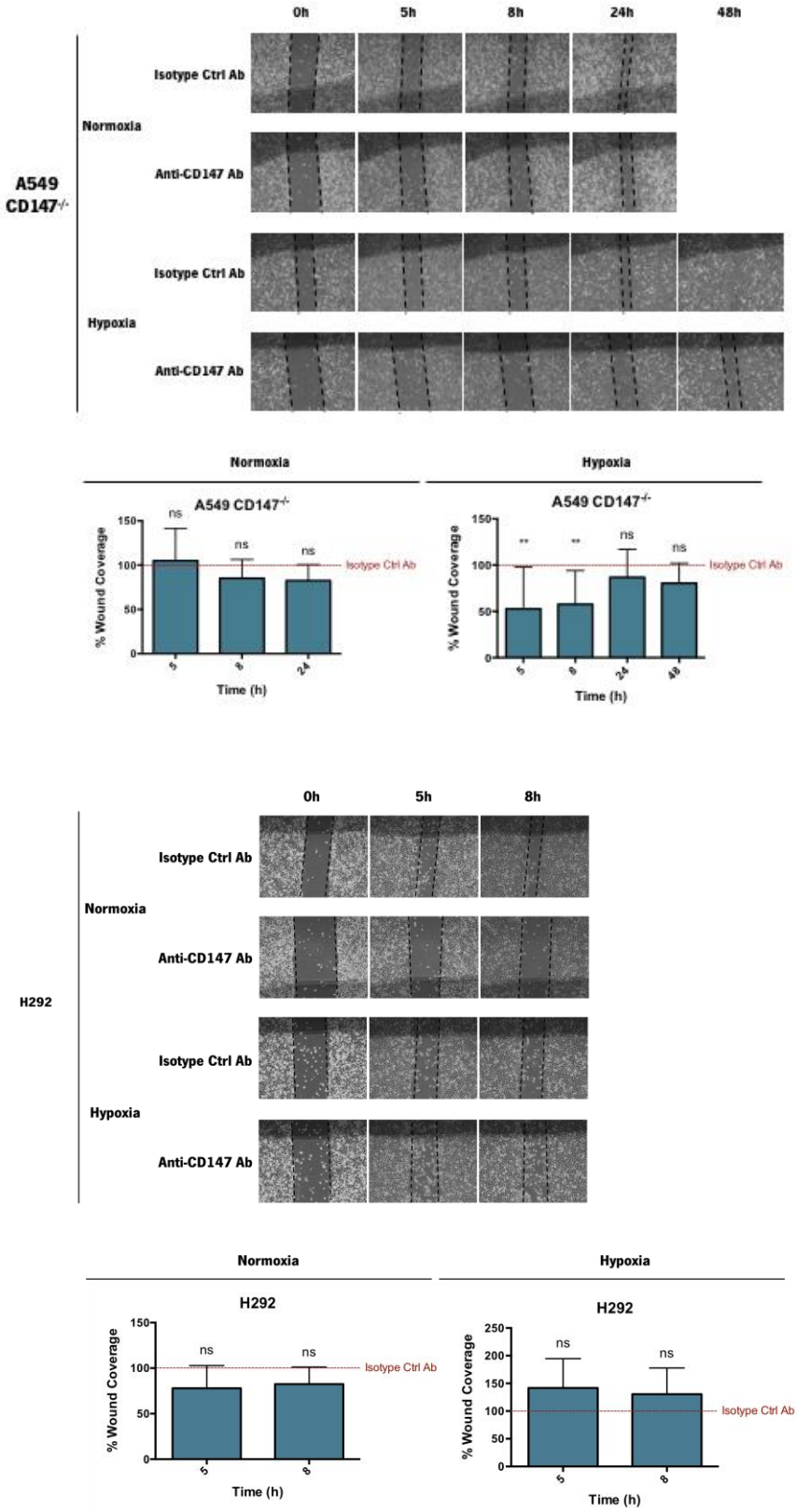

Figure 4.7. Anti-CD147 Ab treatment impaired NSCLC cell migration. Wound-healing assay was performed in A549 WT, A549 CD147$^{-/-}$ and H292 cells to evaluate cell migration upon treatment with 300ng/ml of isotype ctrl or anti-CD147 antibodies under normoxic and hypoxic conditions (magnification:40x; n=2). Results are represented as mean ± standard deviation (ns - not significant; **p< 0.01. Two-way ANOVA post-hoc Sidak's test was applied).

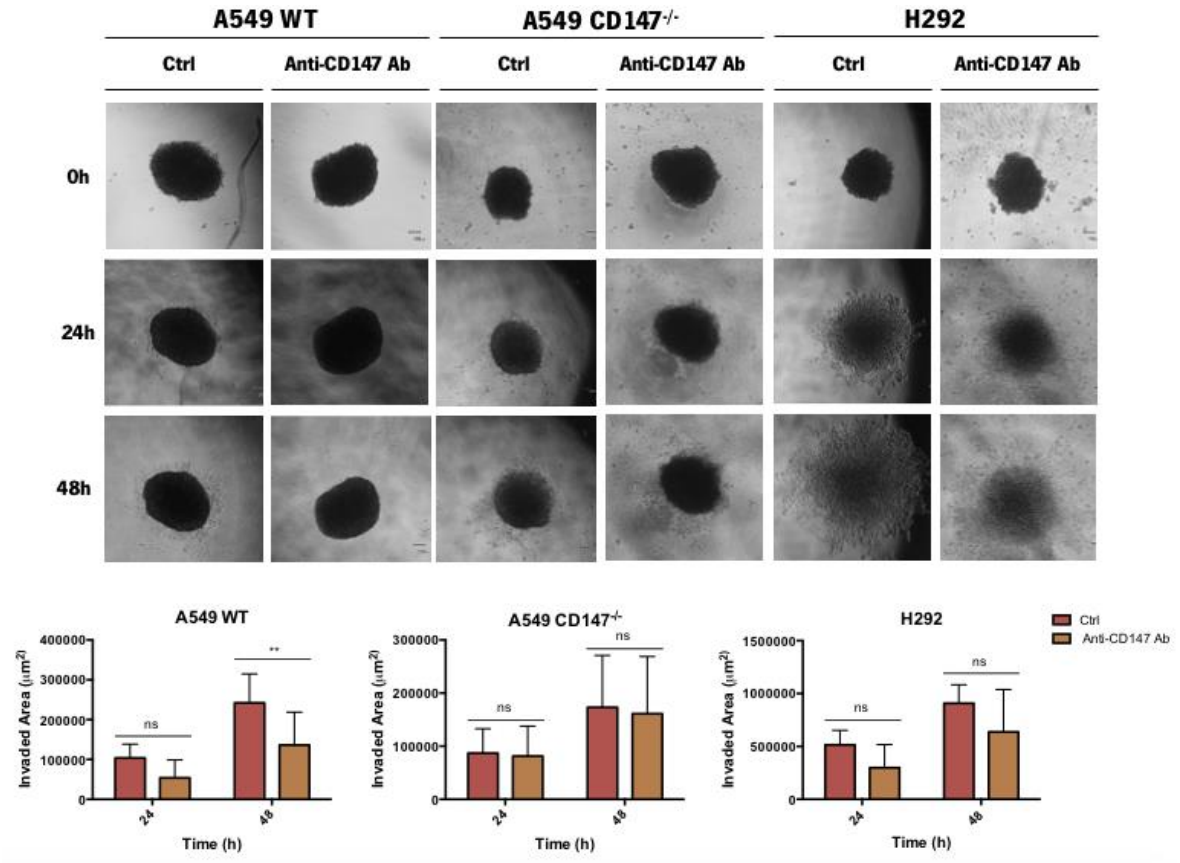

Figure 4.8. Anti-CD147 Ab treatment impaired NSCLC cell invasion. Cell invasion was assessed in A549 WT, A549 CD147$^{-/-}$ and H292 3D-spheroids after 24 and 48 hours of incubation with 300ng/ml anti-CD147 Ab diluted in matrigel (magnification:40x; n=2). Results are represented as mean ± standard deviation (ns - not significant; **p< 0.01. Two-way ANOVA post-hoc Sidak's test was applied).

4.6 LUVs carrying phenformin decreased cell viability and proliferation

As mentioned above, our cell lines showed sensitivity to phenformin, however, the use of this drug on its free form into the human body has been shown to induce severe side effects like lactic acidosis[146]. Thus, we aimed to develop CD147 loaded-liposomes carrying phenformin to specifically introduce this drug in highly CD147 expressed cancer cells and thus, in this way reduce the side effects of phenformin. Liposomes were designed and synthetized on 3B's facilities by our collaborator Doctor Helena Ferreira and underwent an optimization process regarding liposome structure and quantification protocol. During this research project, we received three different samples of LUVs (A, B, C) carrying distinct concentrations of phenformin, which were then reconstituted in cellular medium for the desired concentrations.

The different concentrations of liposomes tested for each sample and the respective concentrations of phenformin incorporated are illustrated in Figure 4.9.

Sample A

[LUVs carrying phenformin] mM	0.01	0.05	0.1	0.2	0.5
[phenformin]µM	0.01	0.07	0.15	0.29	0.73

Sample B

[LUVs carrying phenformin] mM	2	4
[phenformin]µM	105	212

Sample C

[LUVs carrying phenformin] mM	1	2
[phenformin]µM	515	1030

Figure 4.9. The three different samples of LUVs carrying phenformin. Different concentrations of liposomes carrying phenformin from three independent samples and the respective concentrations of phenformin incorporated in the nanocarriers.

Since the liposome quantification method at the beginning of this research project was under optimization, and given the fact that the results between experiments were not coherent, we re-quantified our liposome samples using another quantification method, namely, the Bartlett method[163] and we verified that the original concentrations were not coincident with those that had been previously given to us.

With the liposomes from sample A, we tested the concentration at which liposomes affect A549 WT and H292 cell viability. Our results showed that 0.5mM of liposomes were able to decrease cell viability by cytotoxicity (Figure 4.10A). In parallel, we also evaluated the effect of increasing concentrations of phenformin-loaded liposomes on A549 WT and H292 cell viability. No significant results were observed in both cell lines (Figure 4.10B), suggesting that the concentrations of phenformin inside the nanoparticles were not sufficient to impact on cell viability.

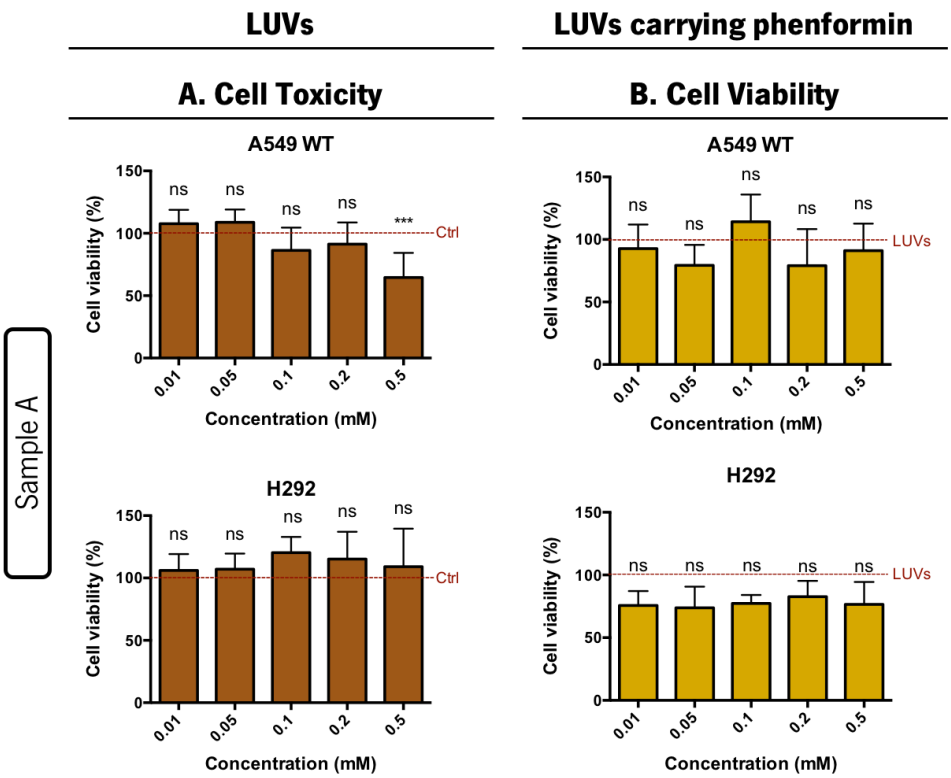

Figure 4.10. LUVs carrying phenformin from sample A did not impair NSCLC cell viability. (A) Toxic effects of LUVs and **(B)** the effect of LUVs carrying phenformin from sample A on A549 WT and H292 cell viability was assessed by SRB assay after 24 hours of incubation under normoxia (n=2). Results are represented as mean ± standard deviation (ns - not significant; ***p<0.001. One-way ANOVA post-hoc Dunnett's test was applied in cell toxicity and viability assays).

As the concentrations of phenformin inside the nanocarriers did not show any impact on NSCLC cell viability, we decided to increase the concentrations of the biguanide drug inside the next sample of liposomes.

When we received liposomes from sample B, we went to confirm whether 0.5mM or higher concentrations (1mM and 2mM) of liposomes were toxic for the cells. After incubating cells with liposomes from sample B, we verified under the microscope that the concentrations of LUVs that we tested seemed to be higher than we expected (Figure 8.1, Annex1). We thought that maybe the concentrations that were given to us were not quantified correctly and thus, we sent our samples to our collaborators and they re-quantified them with other liposome quantification method (*i.e.* Bartlett method). Once re-quantified, we concluded that the original concentrations of liposomes from sample B that we tested were 2mM, 4mM and 8mM. This method revealed to be more reliable than the kit that we used to determine the phospholipid concentration since the following results seemed to be more consistent. Therefore, and considering our results, we concluded that at least up to 2mM, it seemed that liposomes did not exhibit toxic effects to the cells. These results were confirmed with the liposomes from sample C (Figure 4.11A). As previously, we also evaluated the effect of increasing concentrations of phenformin-loaded liposomes

on cell viability and also on cell proliferation. As mentioned above, we increased the concentration of phenformin within the liposomes in sample B. We noted a decrease trend on cell viability and proliferation upon treatment with liposomes carrying 105μM and 212μM of phenformin. In the last sample, we slightly increased the concentrations of phenformin enclosed by the nanosystems and we observed a significant decrease in cell viability in both cell lines upon treatment with at least 515μM of phenformin. Regarding the cell proliferation assay, it seemed that H292 cell proliferation was impaired using both concentrations of phenformin-loaded nanocarriers until 24h, whereas in A549 WT cells this effect was only observed after 48h (Figure 4.11B and C).

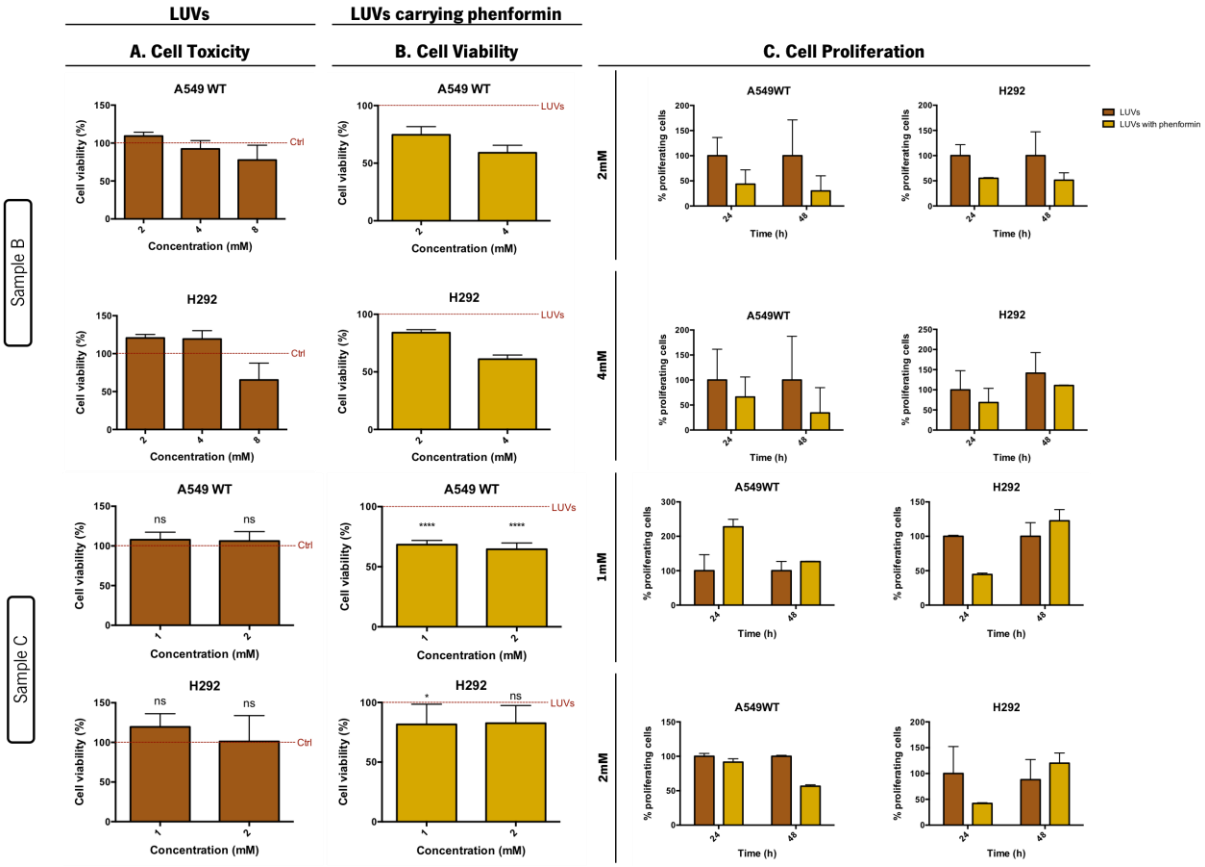

Figure 4.11. LUVs carrying phenformin decreased NSCLC cell viability and proliferation. (A) Toxic effects of LUVs and **(C)** the effect of LUVs carrying phenformin on A549 WT and H292 cell viability was assessed by SRB assay after 24 hours of incubation under normoxia (n=1 for sample B and n=2 for sample C). **(D)** The effect of LUVs carrying phenformin on A549 WT and H292 cell proliferation was evaluated 24 and 48 hours of incubation by BrdU assay (n=1). Results are represented as mean ± standard deviation (ns - not significant; *p< 0.05; ****p<0.0001. One-way ANOVA post-hoc Dunnett's test was applied in cell toxicity and viability assays).

Following these results, we went to verify if the amount of phenformin loaded in the nanocarriers was able to inhibit OXPHOS and consequently, increase glycolytic flux and lactate production in A549 WT and H292 cells. In sample B, we observed that 212μM of phenformin were able to increase the quantity of lactate in the extracellular medium of both cell lines

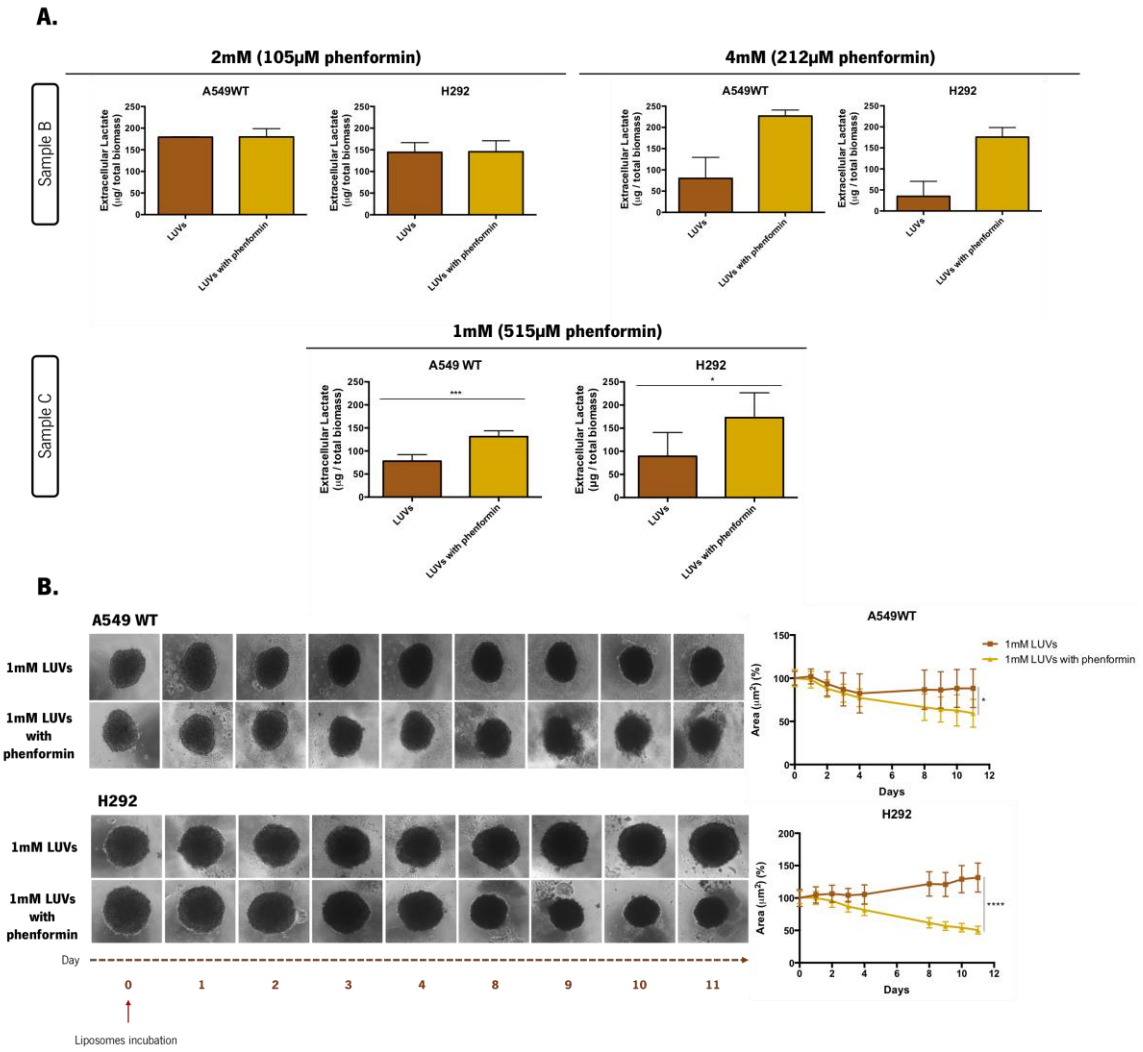

Figure 4.12. LUVs carrying phenformin induced lactate production and decreased 3D-cell growth in NSCLC cells. (A) Extracellular lactate was quantified in A549 WT and H292 cells, after 24 hours of incubation with 2 and 4mM of liposomes carrying phenformin from sample B (n=1) and 1mM from sample C (n=2) under normoxia, using a commercial enzymatic colorimetric kit. **(B)** A549 WT and H292 3D-spheroids growth was analyzed for 11 days after treatment with 1mM LUVs carrying phenformin from sample C (representative images are shown; magnification: 40x; n=2). Results are represented as mean ± standard deviation (*p<0.05; ***p< 0.001; ****p<0.0001. Unpaired two-tailed t-test was applied in the extracellular lactate quantification assay and two-way ANOVA post-hoc Sidak's test in 3D-spheroids growth assay).

. In accordance, with sample C, 515μM significantly induced lactate production, suggesting that phenformin is indeed inhibiting the complex I of the respiratory chain and shift the cell metabolism to the glycolytic pathway (Figure 4.12A).

Since we observed that 515μM of phenformin loaded in 1mM of liposomes significantly reduced cell viability and induced lactate extrusion, we evaluated the effect of these nanocarriers in a 3D-cell culture model (Figure 4.12B). LUVs carrying phenformin were able to significantly decrease A549 WT and H292 3D-spheroid growth.

4.7 Anti-CD147 LUVs carrying phenformin were internalized by A549 WT cells

Upon optimization of the optimal concentration of LUVs alone or carrying phenformin, we next tested the effect of CD147-loaded LUVs carrying phenformin. For that, liposomes were synthesized in accordance with Figure 3.1. These LUVs were formed with 500nM of anti-CD147 Ab and with 200μM of phenformin. Once synthesized, we evaluated A549 WT 3D-spheroid growth upon treatment with 1mM of anti-CD147 liposomes carrying phenformin for 10 days. The results showed that the concentration of phenformin within the nanoparticles was not able to decrease A549 WT-spheroid size over the time (Figure 4.13A).

In order to test if LUVs were being internalized in a 3D-spheroid tumor mass and enter tumor cells, at the end of the experiment, we collected the spheroids, performed immunofluorescence and spheres were observed by confocal microscopy. Liposomes were composed by NBD-cholesterol that stained green which allowed to detect LUVs. We confirmed that these nanocarriers were being internalize by A549 WT cells (green staining), although the anti-CD147 Ab was retained at the cell surface of the peripheral cells of tumor spheroids (red staining) (Figure 4.13B).

A.

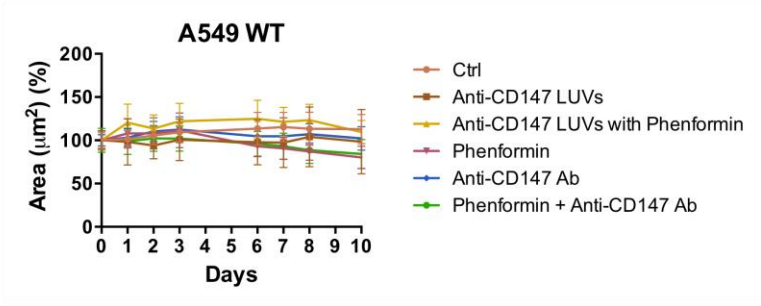

B.

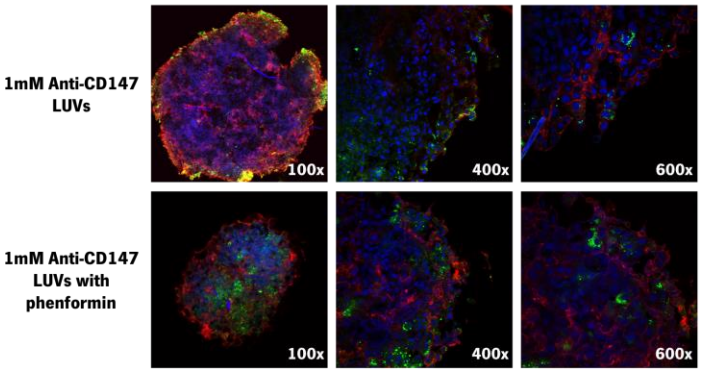

Figure 4.13. LUVs carrying phenformin induced lactate production in NSCLC cells. (A) A549 WT and H292 3D-spheroids growth was analyzed for 10 days after treatment with 1mM of anti-CD147 LUVs carrying phenformin (n=1). **(B)** Immunofluorescence analysis of A549 WT cells after 10 days of treatment with anti-CD147 LUVs carrying or not phenformin (n=1). Images were taken at the identified magnifications (DAPI (Blue) - nuclei; NBD-cholesterol (Green) – LUVs; Alexa Fluor 594 anti-mouse (Red) – Binds to anti-CD147 Ab on the surface of LUVs). Results are represented as mean ± standard deviation.

Chapter 5

DISCUSSION

5. DISCUSSION

Lung cancer became the biggest cancer killer of men worldwide and in some regions of the world, it is also the main cause of cancer-related deaths in women[7]. Although the development of personalized therapies with a view on specific molecular targets has helped to improve the survival of the patients, the overall five-year survival rates remain poor[26]. Therefore, the search for new therapeutic targets and advances on lung cancer treatments are needed.

Most cancers, including lung malignancies are characterized by an exorbitant glycolytic phenotype to generate energy and metabolic intermediates, even in high oxygen tension[43]. This metabolic reprogramming was associated with tumor aggressiveness namely, acidity, invasion and metastization[45]. Several therapies targeting the glycolytic pathway have already entered human trials however, the high plasticity of tumor cells remains a hindrance[144]. Therefore, it is crucial to develop potent anticancer drugs that will inhibit more than one bioenergetic pathway. In this sense, our group recently published that knock-out of CD147 combined with a mitochondrial inhibitor, such as phenformin, lead to a drastic decrease in cell growth *in vitro* and, more importantly, in tumor growth *in vivo*[67]. In this regard, we decided to design and create a new therapeutic approach based on CD147-targeted liposomes carrying phenformin that aims to block simultaneously the major bioenergetic pathways, glycolysis and oxidative phosphorylation in CD147-overexpressing lung cancers.

As a first approach, we characterized the expression of proteins involved in the lactate extrusion and the maintenance of glycolysis rates in human lung cancer cell lines. By western blot and immunofluorescence analysis, we confirmed the expression of monocarboxylate transporters 1/4 and their chaperone CD147 at the plasma membrane and cytosol of A549 and H292 parental cells (Figure 4.1A and B). These results were in agreement with our previous published data and other CD147-related studies that demonstrate that cancer cells overexpress MCTs and CD147[67,77,168,169]. Consistent with genetic studies, their expression was augmented under hypoxia (Figure 4.1A and B). In fact, MCT4 and CD147 promoter regions contain HIF1-α-response elements[63,98]. Although no binding sites for this transcriptional factor were found in MCT1 promoter, it was also reported that its expression is increased by hypoxic conditions in a HIF-1α independent way[168]. Furthermore, in A549 CD147$^{-/-}$ cells, MCT1/4 expression was abolished in both normoxic and hypoxic conditions. These data are in accordance with several reports that demonstrated CD147 inhibition was associated with a downregulation with both MCT1 and MCT4 isoforms[67,77,170].

Before the development and the evaluation of the efficacy of functionalized CD147-targeted liposomes carrying phenformin on non-small cell lung cancer cells, we characterized the anti-tumor effect of phenformin and of the Leaf™ Purified Anti-Human CD147 antibody (anti-CD147 Ab).

Firstly, we investigated whether the non-small cell lung cancer cells respond to the complex I mitochondrial inhibitor, phenformin[149]. As we previously reported[67], all cell lines exhibited high sensitivity to phenformin in a dose-dependent manner. Moreover, IC_{50} values indicated that H292 cells were slightly more sensitive to this biguanide drug than A549 WT cells (Figure 4.2A). A possible explanation for these results is the fact that, H292 cell metabolism could also rely on glutaminolysis since it was reported that H292 present higher glutaminase activity, an metabolic enzyme which catalyzes the conversion of glutamine into glutamate and ammonia, than A549 cells[171]. Indeed, it was described that cancer cells have a heavy demand for glutamine amino-acid[172]. To validate this hypothesis, it will be important to analyze the consumption of this biomolecule in both cell lines.

We next characterized the effect of phenformin alone on A549 and H292 oxidative phosphorylation. Since blockage of OXPHOS increases glycolysis and, consequently, increases lactate production, we measured the extracellular levels of lactate in the supernatant of cells treated with this biguanide. A trend to increase acid lactic production was observed (Figure 4.2B), suggesting that phenformin was able to inhibit the complex I of the mitochondria, compromising the respiration chain functionality and switch cell metabolism to the glycolytic pathway, which is consistent to what was previously described[164]. To validate the anti-cancer effect of phenformin, we evaluated its effect in A549 WT and H292 3D-spheroid growth. According to the 2D-cell culture studies, these results showed a significant decrease in tumor-spheroid size throughout the time (Figure 4.2C). Altogether, phenformin demonstrated to be a putative drug to include in nanoparticles since it showed a potent effect against lung malignancies.

The next question addressed was whether Leaf™ Purified Anti-Human CD147 antibody could specifically target and inhibit CD147 protein at the surface of NSCLC cells. This antibody demonstrated to be specific for CD147 since it recognized this protein in CD147-positive cells and not in CD147 KO cells (Figure 4.3A). Unfortunately, it was not able to impair A549 and H292 cell viability (Figure 4.3C) and lactate extrusion (Figure 4.4A). Due to the highly plasticity of cancer cells in switching their cellular metabolism upon blockage, we went to observed if blocking OXPHOS could sensitize cells to the anti-CD147 Ab. For that, we treated lung cancer cells with both drugs and we analyzed their effect on cell viability and lactate production. Unfortunately, the decrease in cell viability and the quantity of extracellular lactate (Figures 4.5A and B) that we observed were due to the effect of phenformin. These findings

suggest that this antibody was not capable to inhibit CD147 function as a chaperone protein, and consequently, it did not compromise MCT1 and 4 activities.

CD147 is a multifunctional transmembrane glycoprotein[78,79]. Besides its role as MCTs chaperone, CD147 interacts with different molecules playing a role in various physiological and pathological processes, such as cell proliferation, migration and invasion[84]. Indeed, CD147 is known to bind to cyclophilin A secreted by endothelial cells, which induces ERK1/2 and p38 signals that stimulate cell proliferation and colonization[173]. Furthermore, the interaction of CD147 with $\alpha 6\beta 1$ and $\alpha 3\beta 1$ integrins is known to mediate cell migration and invasion via $\alpha 3\beta 1$ integrin-focal adhesion kinase (FAK)-paxilin and FAK-PI3K-Ca^{2+} pathways[84]. CD147 also enhances the production of MMPs and the major constituent of the extracellular matrix, hyaluronan (HA), in order to assist cell migration and invasion. Actually, CD147 stimulates the interaction between hyaluronan and its receptor CD44 and induces the activation of multiple signaling pathways, such as EGFR and Ras/ERK, which are frequently deregulated in cancer. Besides that, it is known that CD147-induced hyaluronan stabilizes and enhances the activity of the lipid-raft associated supramolecular complex CD44/CD147/MCTs/EGFR. The disruption of HA-CD44 interaction by small HA oligosaccharides or knockdown of CD44 attenuated the activation of EGFR/ERK signaling and suppressed the MCT function[174–176].

Thus, we thought that, perhaps this antibody could be acting in an Ig-domain epitope of CD147 that would compromise its function as cell proliferation and migration promoter and an MMP-inducer. Bearing this in mind, we studied the effect of anti-CD147 antibody on these NSCLC cell features.

In accordance with the previous results, the decrease in cell proliferation that we observed was due to phenformin and not due to anti-CD147 Ab treatment (Figure 4.6A), even when we pre-stimulated cells with this antibody (Figure 4.6B).

Unexpectedly, our data revealed a significant decrease in both A549 parental and CD147-null cell migration under treatment with this antibody (Figure 4.7). In fact, it was described that CD147 silencing in A549 cells decreased their capacity to migrate[177]. Moreover, a study in cutaneous squamous cell carcinoma demonstrated that CD147 inhibition decreased cell migration by downregulation of EGFR pathway[167]. Another investigation in human hepatoma cells (HHC), demonstrated that the CD147 silencing resulted in a decrease in HHC cell motility by up-regulation of p190-B RhoGAP[178]. Thus, cell migration assay upon treatment with the neutralizing anti-CD147 antibody has to be repeated to confirm the previously obtained results.

Curiously, a significant reduction in cell invasion was observed for A549 WT cells. Although we did not find significant results for H292 cells, it was possible to observe a trend to decrease cell invasion for

this cell line (Figure 4.8). These data is in accordance to Amit-Choen et al. investigation, in which they demonstrated that this antibody was able to decrease the MMP-9 secretion in co-cultures of renal and breast carcinoma cell lines with monocytic-like cell lines[179], suggesting that it is able to diminish cancer cell invasion. Thus, in the future, we must evaluate the effect of this antibody in MMP production and activity.

Given the therapeutic relevance of phenformin and anti-CD147 antibody on lung cancer 2D and 3D cell growth and on cell migration and invasion, respectively, we next developed CD147-targeted liposomes carrying phenformin and tested its efficacy to eradicate cancer cells.

In the last years, nanotechnology has gained an increased attention and has been intensely exploited to improve conventional cancer therapies. Recently, several nanocarriers have been approved or are undergoing clinical trials, such as Abraxane (albumin-bound paclitaxel nanoparticles), Myocet (non-PEGylated doxorubicin liposomes), Doxil/Caelys (PEGylated doxorubicin liposomes), DaunoXome (daunorubicin liposomes) and Onco TCS (vincristine liposomes)[180].

Within nanocarriers, liposomes have been the most widely applied clinically, owing to their size, biodegradable and biocompatible composition and favorable pharmacokinetic profile[159,160]. The adverse effects of conventional chemotherapeutics can be substantially ameliorated by incorporating the desired chemotherapeutic agent inside these nanocarriers. In this regard, we hypothesized that formulating phenformin into liposomes would enhance its anti-cancer effect and reduce its toxic effects, particularly, in the liver. As mentioned before, these effects are attributed to the fact that phenformin passes through biological membranes by passive diffusion, contrarily to other biguanides that require active transporters[147]. In this context, Krishnamurthy and its collaborators developed phenformin-loaded polymeric micelles and showed that they had a greater anti-tumor efficacy than free phenformin, without inducing liver damage[181]. Although drug-loaded liposomes have already achieved significant advances, the anti-tumor effect of a chemotherapeutic agent can be enhanced by ligand-mediated targeting[180]. In this sense, we coated the liposomes with anti-CD147 antibodies in order to augment their selectivity to CD147-expressing cancer cells and to avoid a systemic effect of phenformin. Besides that, with these immunoliposomes, we intended to inhibit the glycolytic pathway by impairing the MCT1/4 and CD147 association and, thus, preventing the metabolic switch of cancer cells to this pathway. Actually, some researchers have tried to construct CD147 antibody-conjugated immunoliposomes in order to enhance selective drug delivery to tumor cells. For instance, Asakura and its collaborators constructed anti-CD147-labeled polymeric micelles that encapsulated a conjugate of doxorubicin with glutathione and they found a specific accumulation of anti-CD147 micelles in CD147-expressing cells. Besides that, the cell death

rate for anti-CD147 micelles was about 3 times higher than for the IgG micelles[182]. Wang et al., developed CD147-targeted doxorubicin-loaded immunoliposomes and they verified these nanocarriers were able to delivery doxorubicin to CD147-overexpressing cancer cells specifically *in vitro* and *in vivo* with more efficacy than the non-targeted controls[183].

Taking into account all these facts, we started by developing and investigating the anti-cancer effect of LUVs carrying phenformin on lung cancer cell behavior. Interestingly, we observed that 1mM of liposomes carrying 515μM of phenformin was able to significant decrease A549 WT and H292 cell viability (Figure 4.11B) without toxic effects (Figure 4.11A). Regarding the cell proliferation assay, these liposomes tended to reduce lung cancer cell proliferative capacity (Figure 4.11C). Moreover, 515μM of phenformin carried in the nanoparticles was able to significantly induce lactate extrusion (Figure 4.12A). Overall, these results suggested that LUVs were being internalized by lung cancer cells and inhibiting OXPHOS. To corroborate these results, we also evaluated the effect of these nanosystems on 3D-cell culture models. As expected, these drug-delivery systems impacted on A549 WT and H292 growth (Figure 4.12B). Afterwards, we also analyzed A549 WT-spheroid growth under treatment with anti-CD147 liposomes carrying phenformin. Since the concentration of phenformin was lower than the last tested, we did not observe differences on 3D-cell growth (Figure 4.13A), suggesting that the concentration of phenformin inside the nanoparticles must be between 200μM and 500μM. More importantly, we confirmed liposome internalization by confocal microscopy (Figure 4.13B). Nevertheless, the anti-CD147 Ab was retained at the cell surface of the peripheral cells of the tumor spheroids. To understand this fact, we must include negative controls in order to know whether the red staining that we observed at the cell surface of peripheral cells is due to the fact that the secondary antibody was not able to infiltrate all the spheroid or if in fact, the anti-CD147 Ab stayed connected to CD147 at the plasma membrane of peripheral cells. If so, we must repeat the immunofluorescence analysis at earlier timepoints of incubation with the anti-CD147 LUVs in order to know if, at least CD147 is being temporary internalized and then, recycled to plasma membrane.

5.1 Future perspectives

Herein, we demonstrated that CD147-targeted liposomes carrying phenformin are a promising therapeutic approach to attack CD147-overexpressing malignancies.

In the future, all the previously cited findings need to be confirmed and additional *in vitro* assays are also required. To corroborate the effect of CD147-targeted liposomes carrying phenformin on cell viability, MTS and trypan blue assays could be performed. Moreover, flux cytometry could be used to evaluate the uptake of glucose by lung cancer cells; seahorse technology to measure the oxygen consumption rates and extracellular acidification rate; and ATP levels could be quantified by luciferin-luciferase bioluminescence assay.

Lastly, to validate the *in vitro* assays, it will be important to inject mice with parental and CD147-null cells and then, test the efficacy of CD147-targeted liposomes carrying phenformin to decrease tumor growth. It is expected that these immunoliposomes carrying phenformin would be able to internalize CD147-expressing cancer cells, however, some side effects can emerge since CD147 is ubiquitously expressed in several types of cells[90–93]. To avoid this artifact and to culminate this project we aim to develop redox-sensitive liposomes to further increase their selectivity to tumor cells and also include gold-nanoparticles in the aqueous compartment to allow diagnosis and to monitor liposomes route in the mouse model using microcomputed tomography.

Chapter 6

CONCLUSIONS

6. CONCLUSIONS

In this research project, we developed CD147-targeted liposomes carrying phenformin and we characterized its efficacy to eliminate CD147-overexpressing cancer cells. First, we validated the therapeutic effect of phenformin on lung cancer cell lines and consequently, identified this biguanide drug as suitable candidate to be incorporated in drug-delivery systems. In addition, we demonstrated that with the neutralizing anti-CD147 antibody, we were able to specifically target CD147 in the surface of a tumor cell and more importantly, we were able to inhibit CD147 function as a cell migration and invasion promoter. Finally, with the development of liposomes carrying phenformin we were able to decrease the concentration of phenformin necessary to impair cancer cell behavior and thus, reduce its toxic effect. Moreover, we showed that CD147-targeted nanocarriers were able to reach and internalize cancer cells.

In summary, we evaluated the therapeutic relevance of both phenformin and anti-CD147 antibody in a series of cancer cell behavior assays and finally, we validated the efficacy of functionalized CD147-targeted liposomes carrying phenformin by presenting strong evidences that they have a potent anti-cancer effect in CD147-positive cells.

Chapter 7

REFERENCES

7. REFERENCES

1. World Health Statistics 2017: Monitoring health for the SDGs, Sustainable Development Goals. 2017.
2. Allemani C, Matsuda T, Di Carlo V, et al. Global surveillance of trends in cancer survival 2000–14 (CONCORD-3): analysis of individual records for 37513025 patients diagnosed with one of 18 cancers from 322 population-based registries in 71 countries. *Lancet*. 2018;391(10125):1023-1075.
3. Ferlay J, Soerjomataram I, Dikshit R, et al. Cancer incidence and mortality worldwide: sources, methods and major patterns in GLOBOCAN 2012. *International Journal of Cancer*. 2014;136(5):359-386.
4. Cancer prevention and control in the context of an integrated approach: report by the secretariat. 2016.
5. Dela Cruz CS, Tanoue LT, Matthay R. Lung cancer: epidemiology, etiology and prevention. *Clinics in Chest Medicine*. 2011;32(4):1-61.
6. Wong MCS, Lao XQ, Ho K-F, Goggins WB, Tse SLA. Incidence and mortality of lung cancer: global trends and association with socioeconomic status. *Scientific Reports*. 2017;7(1):14300.
7. Didkowska J, Wojciechowska U, Manczuk M, Lobaszewski J. Lung cancer epidemiology: contemporary and future challenges worldwide. *Annals of Translational Medicine*. 2016;4(8):150.
8. RORENO. Registo Oncológico Nacional 2010. Instituto Português de Oncologia do Porto Francisco Gentil - EPE, ed. Porto. 2016.
9. Hespanhol V, Parente B, Cunha J, et al. Lung cancer in northern Portugal: a hospital-based study. *Portuguese Journal of Pulmonology*. 2013;19(6):245-251.
10. IARC. Tobacco smoke and involuntary smoking. *IARC Monographs on the Evaluation of Carcinogenic Risks to Humans*. 2004;83:1-1438.
11. Akopyan G, Bonavida B. Understanding tobacco smoke carcinogen NNK and lung tumorigenesis (Review). *International Journal of Oncology*. 2006;29(4):745-752.
12. Belinsky SA, Devereux TR, Maronpot RR, Stoner GD, Anderson MW. Relationship between the formation of promutagenic adducts and the activation of the K-ras protooncogene in lung tumors from A/J mice treated with nitrosamines. *Cancer Research*. 1989;49(19):5305-5311.
13. Denissenko MF, Pao A, Moon-shong T, Pfeifer GP. Preferential formation of benzo[a]pyrene

adducts at lung cancer mutational hotspots in p53. *Science*. 1996;274(5286):430-432.

14. Samet JM, Avila-Tang E, Boffetta P, et al. Lung cancer in never smokers: clinical epidemiology and environmental risk factors. *Clinical Cancer Research*. 2009;15(18):5626-5645.
15. Pesch B, Kendzia B, Gustavsson P, et al. Cigarette smoking and lung cancer – relative risk estimates for the major histological types from a pooled analysis of case-control studies. *International Journal of Cancer*. 2012;131(5):1210-1219.
16. Travis WD, Brambilla E, Nicholson AG, et al. The 2015 World Health Organization classification of lung tumors: impact of genetic, clinical and radiologic advances since the 2004 classification. *Journal of Thoracic Oncology*. 2015;10(9):1243-1260.
17. Knight SB, Crosbie PA, Balata H, Chudziak J, Hussell T, Dive C. Progress and prospects of early detection in lung cancer. *Open Biology*. 2017;7(9):170070.
18. Denisenko T V, Budkevich IN, Zhivotovsky B. Cell death-based treatment of lung adenocarcinoma. *Cell Death and Disease*. 2018;9(2):117.
19. Zappa C, Mousa SA. Non-small cell lung cancer: current treatment and future advances. *Translational Lung Cancer Research*. 2016;5(3):288-300.
20. Pietanza MC, Byers LA, Minna JD, Rudin CM. Small Cell Lung Cancer: Will recent progress lead to improved outcomes? *Clinical Cancer Research*. 2015;21(10):2244-2255.
21. Bunn PA, Minna J, Augustyn A, et al. Small Cell Lung Cancer: Can recent advances in biology and molecular biology be translated into improved outcomes? *Journal of Thoracic Oncology*. 2016;11(4):453-474.
22. Shtivelman E, Hensing T, Simon GR, et al. Molecular pathways and therapeutic targets in lung cancer. *Oncotarget*. 2014;5(6):1392-1433.
23. Wang Y, Schmid-bindert G, Zhou C. Erlotinib in the treatment of advanced non-small cell lung cancer: an update for clinicians. *Therapeutic Advances in Medical Oncology*. 2011;4(1):19-29.
24. Loong HH, Mok K, Leung LKS, Mok TSK. Crizotinib in the management of advanced-stage non-small-cell lung cancer. *Future Oncology*. 2015;11(5):735-745.
25. Odogwu L, Mathieua L, Blumenthala G, et al. FDA approval summary: Dabrafenib and trametinib for the treatment of metastatic non-small cell lung cancers harboring BRAF V600E mutations. *The Oncologist*. 2018;23(6):740-745.
26. Casaluce F, Sgambato A, Maione P, et al. Selumetinib for the treatment of non-small cell lung cancer. *Expert Opinion on Investigational Drugs*. 2017;26(8):973-984. .
27. Hyman DM, Puzanov I, Subbiah V, et al. Vemurafenib in multiple nonmelanoma cancers with

BRAF V600 mutations. *The New England Journal of Medicine*. 2015;373(8):726-736.

28. Morgensztern D, Campo MJ, Dahlberg SE, et al. Molecularly targeted therapies in non-small cell lung cancer annual update 2014. *Journal of Thoracic Oncology*. 2015;10(1 Suppl 1):S1-63.
29. Herbst RS, Morgensztern D, Boshoff C. The biology and management of non-small cell lung cancer. *Nature*. 2018;553(7689):446-454.
30. Hellmann MD, Ciuleanu T-E, Pluzanski A, et al. Nivolumab plus ipilimumab in lung cancer with a high tumor mutational burden. *The New England Journal of Medicine*. 2018;378(22):2093-2104.
31. Scott A, Goldberg SB, Balmanoukian A, et al. Safety and antitumour activity in a phase 1b study of combined checkpoint blockade with anti-PD-L1 (durvalumab) and anti-CTLA4 (tremelimumab) in non-small cell lung cancer. *Lancet Oncology*. 2016;17(3):299-308.
32. Lim SH, Sun J, Lee S, Ahn JS, Park K, Ahn MJ. Pembrolizumab for the treatment of non-small cell lung cancer. *Expert Opinion on Biological Therapy*. 2016;16(3):397-406.
33. Dudnik E, Moskovitz M, Daher S, et al. Effectiveness and safety of nivolumab in advanced non-small cell lung cancer: the real-life data. *Lung Cancer*. 2017.
34. Jean F, Tomasini P, Barlesi F. Atezolizumab: Feasible second-line therapy for patients with non-small cell lung cancer? A review of efficacy, safety and place in therapy. *Therapeutic Advances in Medical Oncology*. 2017;9(12):769-779.
35. Tomasini P, Greillier L, Boyer A, Jeanson A, Barlesi F. Durvalumab after chemoradiotherapy in stage III non-small cell lung cancer. *Journal of Thoracic Disease*. 2018;10(Suppl 9):S1032-S1036.
36. Marciscano AE, Gulley JL. Avelumab demonstrates promise in advanced NSCLC. *Oncotarget*. 2017;8(61):102767-102768.
37. Hanahan D, Weinberg RA. Hallmarks of cancer: the next generation. *Cell*. 2011;144(5):646-674.
38. Deberardinis RJ, Chandel NS. Fundamentals of cancer metabolism. *Science Advances*. 2016;2(5):e1600200.
39. Warburg O. On the origin of cancer cells. *Science*. 1956;123(3191):309-314.
40. Heiden MG Vander, Cantley LC, Thompson CB. Understanding the Warburg effect: the metabolic requirements of cell proliferation. *Science*. 2009;324(5930):1029-1033.
41. Liberti M V, Locasale JW. The Warburg Effect: How does it benefit cancer cells? *Trends in Biochemical Sciences*. 2016;41(3):211-218.
42. Boroughs LK, Deberardinis RJ. Metabolic pathways promoting cancer cell survival and growth. *Nature Cell Biology*. 2015;17(4):351-359.
43. Gatenby RA, Gillies RJ. Why do cancers have high aerobic glycolysis? *Nature Reviews Cancer*.

2004;4(11):891-899.

44. Parks SK, Chiche J, Pouysségur J. Disrupting proton dynamics and energy metabolism for cancer therapy. *Nature Reviews Cancer*. 2013;13(9):611-623.

45. Estrella V, Chen T, Lloyd M, et al. Acidity generated by the tumor microenvironment drives local invasion. *Cancer Research*. 2013;73(5):1524-1535.

46. Daniel C, Bell C, Burton C, Harguindey S, Reshkin SJ, Rauch C. The role of proton dynamics in the development and maintenance of multidrug resistance in cancer. *Biochimica et Biophysica Acta (BBA) - Molecular Basis of Disease*. 2013;1832(5):606-617.

47. Beckert S, Farrahi F, Aslam RS, Scheuenstuhl H, Hussain MZ, Hunt TK. Lactate stimulates endothelial cell migration. *Wound Repair and Regeneration*. 2006;14(3):321-324.

48. Sonveaux P, Copetti T, Saedeleer CJ, et al. Targeting the lactate transporter MCT1 in endothelial cells inhibits lactate-induced HIF-1 activation and tumor angiogenesis. *PLoS ONE*. 2012;7(3):e33518.

49. Végran F, Boidot R, Michiels C, Sonveaux P, Feron O. Lactate influx through the endothelial cell monocarboxylate transporter MCT1 supports an NF-kB/IL-8 pathway that drives tumor angiogenesis. *Cancer Research*. 2011;71(7):2550-2560.

50. Baumann F, Leukel P, Doerfelt A, et al. Lactate promotes glioma migration by TGF-β2–dependent regulation of matrix metalloproteinase-2. *Neuro-oncology*. 2009;11(4):368-380.

51. Marchiq I, Pouysségur J. Hypoxia, cancer metabolism and the therapeutic benefit of targeting lactate/H(+) symporters. *Journal of Molecular Medicine*. 2016;94(2):155-171.

52. Halestrap AP, Denton RM. Specific inhibition of pyruvate transport in rat liver mitochondria and human erythrocytes by α-cyano-4-hydroxycinnamate. *Biochemical Journal*. 1974;138(2):313-316.

53. Poole RC, Halestrap AP. Transport of lactate and other monocarboxylates across mammalian plasma membranes. *American Journal of Physiology*. 1993;264(4 Pt 1):C761-82.

54. Halestrap AP. The SLC16 gene family – structure, role and regulation in health and disease. *Molecular Aspects of Medicine*. 2013;34(2-3):337-349.

55. Halestrap AP, Price NT. The proton-linked monocarboxylate transporter (MCT) family: structure, function and regulation. *Biochemical Journal*. 1999;343(Pt 2):281-299.

56. Pinheiro C, Longatto-Filho A, Azevedo-Silva J, Casal M, Schmitt FC, Baltazar F. Role of monocarboxylate transporters in human cancers: state of the art. *Journal of Bioenergetics and Biomembranes*. 2012;44(1):127-139.

57. Christian D, Meredith HC. The SLC16 monocaboxylate transporter family. *Xenobiotica*. 2008;38(7-8):1072-1106.
58. Grollman EF, Philp NJ, Mcphie P, Ward RD, Sauer B. Determination of transport kinetics of chick MCT3 monocarboxylate transporter from retinal pigment epithelium by expression in genetically modified yeast. *Biochemistry*. 2000;39(31):9351-9357.
59. Halestrap AP, Wilson MC. The monocarboxylate transporter family-role and regulation. *IUBMB Life*. 2012;64(2):109-119.
60. Halestrap AP. The monocarboxylate transporter family — structure and functional characterization. *IUBMB Life*. 2012;64(1):1-9.
61. Hashimoto T, Hussien R, Oommen S, Gohil K, Brooks GA. Lactate sensitive transcription factor network in L6 cells: activation of MCT1 and mitochondrial biogenesis. *The FASEB Journal*. 2007;21(10):2602-2612.
62. Doherty JR, Yang C, Scott KEN, et al. Blocking lactate export by inhibiting the myc target MCT1 disables glycolysis and glutathione synthesis. *Cancer Research*. 2014;74(3):908-920.
63. Ullah MS, Davies AJ, Halestrap AP. The plasma membrane lactate transporter MCT4, but not MCT1, is up-regulated by hypoxia through a HIF-1α-dependent mechanism. *The Journal of Biological Chemistry*. 2006;281(14):9030-9037.
64. Boidot R, Végran F, Meulle A, et al. Regulation of monocarboxylate transporter MCT1 expression by p53 mediates inward and outward lactate fluxes in tumors. *Cancer Research*. 2012;72(4):939-948.
65. Thibault R, De Coppet P, Daly K, et al. Down-regulation of the monocarboxylate transporter 1 is involved in butyrate deficiency during intestinal inflammation. *Gastroenterology*. 2007;133(6):1916-1927.
66. Halestrap AP. Monocarboxylic acid transport. *Comprehensive Physiology*. 2013;3(4):1611-1643.
67. Granja S, Marchiq I, Le Floch R, Moura CS, Baltazar F, Pouysségur J. Disruption of BASIGIN decreases lactic acid export and sensitizes non-small cell lung cancer to biguanides independently of the LKB1 status. *Oncotarget*. 2014;6(9):6708–6721.
68. Le Floch R, Chiche J, Marchiq I, et al. CD147 subunit of lactate/H(+) symporters MCT1 and hypoxia-inducible MCT4 is critical for energetics and growth of glycolytic tumors. *Proceedings of the National Academy of Sciences of the United States of America*. 2011;108(40):16663-16668.
69. Morais-santos F, Granja S, Miranda-gonçalves V, et al. Targeting lactate transport suppresses in vivo breast tumour growth. *Oncotarget*. 2015;6(22):19177–19189.

70. Boasquevisque PH, Schoeneberger V, Caporiccio L, Vellanki RN, Koritzinsky M, Wouters BG. Targeting lactate transporters MCT-1 and MCT-4 to inhibit the growth of hypoxic HNSCC cells in vitro. *International Journal of Radiation Oncology, Biology, Physics*. 2017;99(2):E579.
71. Sonveaux P, Végran F, Schroeder T, et al. Targeting lactate-fueled respiration selectively kills hypoxic tumor cells in mice. *The Journal of Clinical Investigation*. 2008;118(12):3930–3942.
72. Pérez-Escuredo J, Hée VF Van, Sboarina M, et al. Monocarboxylate transporters in the brain and in cancer. *Biochimica et Biophysica Acta (BBA) - Molecular Cell Research*. 2016;1863(10):2481-2497.
73. Baltazar F, Pinheiro C, Morais-Santos F, et al. Monocarboxylate transporters as targets and mediators in cancer therapy response. *Histology and Histopathology*. 2014;29(12):1511-1524.
74. Polanski R, Hodgkinson CL, Fusi A, et al. Activity of the Monocarboxylate Transporter 1 inhibitor AZD3965 in Small Cell Lung Cancer. *Clinical Cancer Research*. 2014;20(4):926-937.
75. Plummer R, Halford S, Jones P, et al. A first-in-human first-in-class (FIC) trial of the monocarboxylate transporter 1 (MCT1) inhibitor AZD3965 in patients with advanced solid tumours. *Annals of Oncology*. 2018;29(Suppl 3).
76. Bola BM, Chadwick AL, Michopoulos F, et al. Inhibition of monocarboxylate transporter-1 (MCT1) by AZD3965 enhances radiosensitivity by reducing lactate transport. *Molecular Cancer Therapeutics*. 2014;13(12):2805-2816.
77. Kendrick AA, Schafer J, Dzieciatkowska M, et al. CD147: a small molecule transporter ancillary protein at the crossroad of multiple hallmarks of cancer and metabolic reprogramming. *Oncotarget*. 2017;8(4):6742-6762.
78. Biswas C. Tumor cell stimulation of collagenase production by fibroblasts. *Biochemical and Biophysical Research Communications*. 1982;109(3):1026-1034.
79. Miyauchi T, Kanekura T, Yamaoka A, Ozawa M, Miyazawa S, Muramatsu T. Basigin, a new, broadly distributed member of the immunoglobulin superfamily, has strong homology with both the immunoglobulin V domain and the beta-chain of major histocompatibility complex class II antigen. *Journal of Biochemistry*. 1990;107(2):316-323.
80. Kaname T, Miyauchi T, Kuwano A, Matsuda Y, Muramatsu T, Kajii T. Mapping basigin (BSG), a member of the immunoglobulin superfamily, to 19p13.3. *Cytogenet Cell Genet*. 1993;64(3-4):195-197.
81. Liao C-G, Kong L-M, Song F, et al. Characterization of basigin isoforms and the inhibitory function of basigin-3 in human hepatocellular carcinoma proliferation and invasion. *Molecular and Cellular*

Biology. 2011;31(13):2591-2604.

82. Hanna SM, Kirk P, Holt OJ, Puklavec MJ, Brown MH, Barclay a N. A novel form of the membrane protein CD147 that contains an extra Ig-like domain and interacts homophilically. *BMC Biochemistry*. 2003;4:17.

83. Belton RJ, Chen L, Mesquita FS, Nowak RA. Basigin-2 is a cell surface receptor for soluble basigin ligand. *Journal of Biological Chemistry*. 2008;283(26):17805-17814.

84. Weidle UH, Scheuer W, Eggle D, Klostermann S, Stockinger H. Cancer-related issues of CD147. *Cancer Genomics and Proteomics*. 2010;7(3):157-169.

85. Wei Tang, Sharon B. Chang and MEH. Links between CD147 function, glycosylation, and Caveolin-1. *Molecular Biology of the Cell*. 2004;15(9):4043-4050.

86. Fossum S, Mallett S, Barclay AN. The MRC OX-47 antigen is a member of the immunoglobulin superfamily with an unusual transmembrane sequence. *European Journal of Immunology*. 1991;21(3):671-679.

87. Seulberger H, Lottspeich F, Risau W. The inducible blood-brain barrier specific molecule HT7 is a novel immunoglobulin-like cell surface glycoprotein. *The EMBO Journal*. 1990;9(7):2151-2158.

88. Biswas C, Zhang Y, DeCastro R, et al. The human tumor cell-derived collagenase stimulatory factor (renamed EMMPRIN) is a member of the immunoglobulin superfamily. *Cancer Research*. 1995;55(2):434-439.

89. Zhao P, Zhang W, Tang J, et al. Annexin II promotes invasion and migration of human hepatocellular carcinoma cells in vitro via its interaction with HAb18G/CD147. *Cancer Science*. 2010;101(2):387-395.

90. Boulos S, Meloni BP, Arthur PG, Majda B, Bojarski C, Knuckey NW. Evidence that intracellular cyclophilin A and cyclophilin A/CD147 receptor-mediated ERK1/2 signalling can protect neurons against in vitro oxidative and ischemic injury. *Neurobiology of Disease*. 2007;25(1):54-64.

91. Kasinrerk W, Fiebiger E, Stefanová I, Baumruker T, Knapp W, Stockinger H. Human leukocyte activation antigen M6, a member of the Ig superfamily, is the species homologue of rat OX-47, mouse basigin, and chicken HT7 molecule. *The Journal of Immunology*. 1992;149(3):847-854.

92. Li S, Nguyen TT, Bonanno JA. CD147 required for corneal endothelial lactate transport. *Investigative Ophthalmology and Visual Science*. 2014;55(7):4673-4681.

93. Ayva SK, Karabulut AA, Akatli AN, Atasoy P, Bozdogan O. Epithelial expression of extracellular matrix metalloproteinase inducer/CD147 and matrix metalloproteinase-2 in neoplasms and precursor lesions derived from cutaneous squamous cells: an immunohistochemical study.

Pathology Research and Practice. 2013;209(10):627-634.

94. Lee A, Rode A, Nicoll A, et al. Circulating CD147 predicts mortality in advanced hepatocellular carcinoma. *Journal of Gastroenterology and Hepatology*. 2016;31(2):459-466.
95. Zhao J, Ye W, Wu J, et al. Sp1-CD147 positive feedback loop promotes the invasion ability of ovarian cancer. *Oncology Reports*. 2015;34(1):67-76.
96. Kong L-M, Liao C-G, Chen L, et al. Promoter hypomethylation up-regulates CD147 expression through increasing Sp1 binding and associates with poor prognosis in human hepatocellular carcinoma. *Journal of Cellular and Molecular Medicine*. 2011;15(6):1415-1428.
97. Dai L, Qin Z, Defee M, Toole B, Kirkwood KL, Parsons C. Kaposi sarcoma-associated herpesvirus (KSHV) induces a functional tumor-associated phenotype for oral fibroblasts. *Cancer Letters*. 2012;318(2):214-220.
98. Ke X, Fei F, Chen Y, et al. Hypoxia upregulates CD147 through a combined effect of HIF-1α and Sp1 to promote glycolysis and tumor progression in epithelial solid tumors. *Carcinogensis*. 2012;33(8):1598-1607.
99. Wu J, Ru N, Zhang Y, et al. HAb18G/ CD147 promotes epithelial-mesenchymal transition through TGF-β signaling and is transcriptionally regulated by Slug. *Oncogene*. 2011;30(43):4410-4427.
100. Fu T, Chang C, Lin C, et al. Let-7b-mediated suppression of basigin expression and metastasis in mouse melanoma cells. *Experimental Cell Research*. 2011;317(4):445-451.
101. Zhang Z, Zhang Y, Sun X, Ma X, Chen Z. microRNA-146a inhibits cancer metastasis by downregulating VEGF through dual pathways in hepatocellular carcinoma. *Molecular Cancer*. 2015;14(5):1-15.
102. Kong L, Liao C, Zhang Y, et al. A regulatory loop involving miR-22, Sp1, and c-Myc modulates CD147 expression in breast cancer invasion and metastasis. *Cancer Research*. 2014;74(14):3764-3778.
103. Peng L, Zhu H, Wang J, et al. MiR-492 is functionally involved in Oxaliplatin resistance in colon cancer cells LS174T via its regulating the expression of CD147. *Molecular and Cellular Biochemistry*. 2015;405(1-2):73-79.
104. Hagemann T, Wilson J, Kulbe H, et al. Macrophages induce invasiveness of epithelial cancer cells via NF-kB and JNK. *The Journal of Immunology*. 2005;175(2):1197-1205.
105. Venkatesan B, Valente AJ, Reddy VS, Siwik DA, Chandrasekar B. Resveratrol blocks interleukin-18-EMMPRIN cross-regulation and smooth muscle cell migration. *American Journal of Physiology-Heart and Circulatory Physiology*. 2009;297(2):874-886.

106. Rucci N, Millimaggi D, Mari M, et al. Receptor activator of NF-kB ligand enhances breast cancer – induced osteolytic lesions through upregulation of extracellular matrix metalloproteinase inducer/ CD147. *Cancer Research*. 2010;70(15):6150-6160.

107. Braundmeier AG, Fazleabas AT, Lessey BA, Guo H, Toole BP, Nowak RA. Extracellular matrix metalloproteinase inducer regulates metalloproteinases in human uterine endometrium. *The Journal of Clinical Endocrinology and Metabolism*. 2006;91(6):2358-2365.

108. Chen L, Bi J, Nakai M, Bunick D, Couse JF, Korach KS NR. Expression of basigin in reproductive tissues of oestrogen receptor-α or -β null mice. *Reproduction*. 2010;139(6):1057-1066.

109. Fanelli A, Grollman EF, Wang D, Philp NJ. MCT1 and its accessory protein CD147 are differentially regulated by TSH in rat thyroid cells. *American Journal of Physiology-Endocrinology and Metabolism*. 2003;285(6):E1223-1229.

110. Egawa N, Koshikawa N, Tomari T, Nabeshima K, Isobe T, Seiki M. Membrane type 1 matrix metalloproteinase (MT1-MMP/MMP-14) cleaves and releases a 22-kDa extracellular matrix metalloproteinase inducer (EMMPRIN) fragment from tumor cells. *The Journal of Biological Chemistry*. 2006;281(49):37576-37585.

111. Tang Y, Kesavan P, Nakada MT, Yan L. Tumor-stroma interaction: positive feedback regulation of extracellular matrix metalloproteinase inducer (EMMPRIN) expression and matrix metalloproteinase-dependent generation of soluble EMMPRIN. *Molecular Cancer Research*. 2004;2(2):73-80.

112. Gallagher SM, Castorino JJ, Wang D, Philp NJ. Monocarboxylate transporter 4 regulates maturation and trafficking of CD147 to the plasma membrane in the metastatic breast cancer cell line MDA-MB-231. *Cancer Research*. 2007;67(9):4182-4189.

113. Doherty JR, Cleveland JL. Targeting lactate metabolism for cancer therapeutics. *The Journal of Clinical Investigation*. 2013;123(9):3685-3692.

114. Zhang W, Zhao P, Xu X, et al. Annexin A2 promotes the migration and invasion of human hepatocellular carcinoma cells in vitro by regulating the shedding of CD147-harboring microvesicles from tumor cells. *PLoS ONE*. 2013;8(8):e67268.

115. Pushkarsky T, Yurchenko V, Vanpouille C, et al. Cell surface expression of CD147/ EMMPRIN is regulated by cyclophilin 60. *The Journal of Biological Chemistry*. 2005;280(30):27866-27871.

116. Grass GD, Toole BP. How, with whom and when: an overview of CD147-mediated regulatory networks influencing matrix metalloproteinase activity. *Bioscience Reports*. 2016;36(1):e00283.

117. Kanekura T, Miyauchi T, Tashiro M, Muramatsu T. Basigin, a new member of the immunoglobulin

superfamily: genes in different mammalian species, glycosylation changes in the molecule from adult organs and possible variation in the N-terminal sequences. *Cell Structure and Function*. 1991;16(1):23-30.

118. Igakura T, Kadomatsu K, Kaname T, et al. A null mutation in basigin, an immunoglobulin superfamily member, indicates its important roles in peri-implantation development and spermatogenesis. *Developmental Biology*. 1998;194(2):152-165.
119. Ochrietor JD, Moroz TM, Kadomatsu K, Muramatsu T, Linser PJ. Retinal degeneration following failed photoreceptor maturation in 5A11/basigin null mice. *Experimental Eye Research*. 2001;72(4):467-477.
120. Berditchevski F, Chang S, Bodorova J, Hemler ME. Generation of monoclonal antibodies to integrin-associated. *The Journal of Biological Chemistry*. 1997;272(46):29174-29180.
121. Yurchenko V, Constant S, Bukrinsky M. Dealing with the family: CD147 interactions with cyclophilins. *Immunology*. 2006;117(3):301-309.
122. Iacono KT, Brown AL, Greene MI, Saouaf SJ. CD147 immunoglobulin superfamily receptor function and role in pathology. *Experimental and Molecular Pathology*. 2007;83(3):283-295.
123. Naruhashi K, Kadomatsu K, Igakura T, et al. Abnormalities of sensory and memory functions in mice lacking Bsg gene. *Biochemical and Biophysical Research Communications*. 1997;236(3):733-737.
124. Peng C, Zhang S, Lei L, et al. Epidermal CD147 expression plays a key role in IL-22-induced psoriatic dermatitis. *Scientific Reports*. 2017;7:44172.
125. Pushkarsky T, Zybarth G, Dubrovsky L, et al. CD147 facilitates HIV-1 infection by interacting with virus-associated cyclophilin A. *Proceedings of the National Academy of Sciences of the United States of America*. 2001;98(11):6360-6365.
126. Crosnier C, Bustamante LY, Bartholdson SJ, et al. Basigin is a receptor essential for erythrocyte invasion by plasmodium falciparum. *Nature*. 2011;480(7378):534-537.
127. Zhou S, Zhou H, Walian PJ, Jap BK. CD147 is a regulatory subunit of the γ-secretase complex in Alzheimer's disease amyloid β-peptide production. *Proceedings of the National Academy of Sciences of the United States of America*. 2005;102(21):7499-7504.
128. Xiong L, Edwards CK, Zhou L. The biological function and clinical utilization of CD147 in human diseases: a review of the current scientific literature. *International Journal of Molecular Sciences*. 2014;15(10):17411-17441.
129. Li H, Wu D, Shi S, et al. Expression and clinical significance of CD147 in renal cell carcinoma: a

meta-analysis. *Oncotarget*. 2017;8(31):51331-51344.

130. Li H, Xi Z, Dai X, et al. CD147 and glioma: a meta-analysis. *Journal of Neuro-Oncology*. 2017;134(1):145-156.
131. Peng F, Li H, Ning Z, et al. CD147 and prostate cancer: a systematic review and meta-analysis. *PLoS ONE*. 2016;11(9):e0163678.
132. Peng F, Li H, You Q, et al. CD147 as a novel prognostic biomarker for hepatocellular carcinoma: a meta-analysis. *BioMed Research International*. 2017;2017:5019367.
133. Hu C, Dong X, Wu J, et al. CD147 overexpression may serve as a promising diagnostic and prognostic marker for gastric cancer: evidence from original research and literature. *Oncotarget*. 2017;8(19):30888-30899.
134. Yan L, Zucker S, Toole BP. Roles of the multifunctional glycoprotein, emmprin (basigin; CD147), in tumour progression. *Journal of Thrombosis and Haemostasis*. 2005;93(2):199-204.
135. Slomiany MG, Grass GD, Robertson AD, et al. Hyaluronan, CD44, and emmprin regulate lactate efflux and membrane localization of monocarboxylate transporters in human breast carcinoma cells. *Cancer Research*. 2009;69(4):1293-1301.
136. Khayati F, Pérez-cano L, Maouche K, Sadoux A. EMMPRIN/CD147 is a novel coreceptor of VEGFR-2 mediating its activation by VEGF. *Oncotarget*. 2015;6(12):9766-9780.
137. Manoharan C, Wilson MC, Sessions RB, Halestrap AP. The role of charged residues in the transmembrane helices of monocarboxylate transporter 1 and its ancillary protein basigin in determining plasma membrane expression and catalytic activity. *Molecular Membrane Biology*. 2006;23(6):486-498.
138. Wu J, Hao Z, Zhao Y, et al. Full-length soluble CD147 promotes MMP-2 expression and is a potential serological marker in detection of hepatocellular carcinoma. *Journal of Translational Medicine*. 2014;12:190.
139. Knutti N, Kuepper M, Friedrich K. Soluble extracellular matrix metalloproteinase inducer (EMMPRIN, EMN) regulates cancer-related cellular functions by homotypic interactions with surface CD147. *The FEBS Journal*. 2015;282(21):4187-4200.
140. Xu J, Xu H, Zhang Q, et al. HAb18G/CD147 functions in invasion and metastasis of hepatocellular carcinoma. *Molecular Cancer Research*. 2007;5(6):605-614.
141. Xu J, Shen Z, Chen X, et al. A randomized controlled trial of licartin for preventing hepatoma recurrence after liver transplantation. *Hepatology*. 2007;45(2):269-276.
142. Dean NR, Newman JR, Helman EE, et al. Anti-EMMPRIN monoclonal antibody as a novel agent

for therapy of head and neck cancer. *Clinical Cancer Research*. 2009;15(12):4058-4065.

143. Fu Z, Wang L, Cui H, et al. A novel small-molecule compound targeting CD147 inhibits the motility and invasion of hepatocellular carcinoma cells. *Oncotarget*. 2016;7(8):9429–9447.
144. Kroemer G, Pouyssegur J. Tumor cell metabolism: cancer's Achilles' heel. *Cancer Cell*. 2008;13(6):472-482.
145. McKendry JBR, Kuwayti K, Rado PP. Clinical experience with DBI (phenformin) in the management of diabetes. *Canadian Medical Association Journal*. 1959;80(10):773-778.
146. McGuinness ME, Talbert RL. Phenformin-induced lactic acidosis: a forgotten adverse drug reaction. *Annals of Pharmacotherapy*. 1993;27(10):1183-1187.
147. Pollak M. Potential applications for biguanides in oncology. *Journal of Clinical Investigation*. 2013;123(9):3693-3700.
148. Huang X, Wullschleger S, Shpiro N, et al. Important role of the LKB1–AMPK pathway in suppressing tumorigenesis in PTEN-deficient mice. *Biochemical Journal*. 2008;412(2):211-221.
149. Owen MR, Doran E, Halestrap AP. Evidence that metformin exerts its anti-diabetic effects through inhibition of complex 1 of the mitochondrial respiratory chain. *Biochemical Journal*. 2000;348(Pt 3):607-614.
150. Bridges HR, Sirviö VA, Agip AA, Hirst J. Molecular features of biguanides required for targeting of mitochondrial respiratory complex I and activation of AMP-kinase. *BMC Biology*. 2016;14(65):1-11.
151. Jackson AL, Sun W, Kilgore J, et al. Phenformin has anti-tumorigenic effects in human ovarian cancer cells and in an orthotopic mouse model of serous ovarian cancer. *Oncotarget*. 2017;8(59):100113-100127.
152. Liu Z, Ren L, Liu C, Xia T, Zha X, Wang S. Phenformin induces cell cycle change, apoptosis, and mesenchymal-epithelial transition and regulates the AMPK/ mTOR/ p70s6k and MAPK/ ERK pathways in breast cancer cells. *PLoS ONE*. 2015;10(6):e0131207.
153. Dilman VM, Anisimov VN. Effect of treatment with phenformin, diphenylhydantoin or L-dopa on life span and tumour incidence in C3H/Sn mice. *Gerontology*. 1980;26(5):241-246.
154. Rajeshkumar N V, Yabuuchi S, Pai SG, et al. Treatment of pancreatic cancer patient-derived xenograft panel with metabolic inhibitors reveals efficacy of phenformin. *Clinical Cancer Research*. 2017;23(18):5639-5647.
155. Dykens JA, Jamieson J, Marroquin L, Nadanaciva S, Billis PA, Will Y. Biguanide-induced mitochondrial dysfunction yields increased lactate production and cytotoxicity of aerobically-poised

HepG2 cells and human hepatocytes in vitro. *Toxicology and Applied Pharmacology*. 2008;233(2):203-210.

156. Zhang J, Nannapaneni S, Wang D, et al. Phenformin enhances the therapeutic effect of selumetinib in KRAS-mutant non-small cell lung cancer irrespective of LKB1 status. *Oncotarget*. 2017;8(35):59008-59022.
157. Guo Z, Zhao M, Howard EW, et al. Phenformin inhibits growth and epithelial-mesenchymal transition of ErbB2-overexpressing breast cancer cells through targeting the IGF1R pathway. *Oncotarget*. 2017;8(36):60342-60357.
158. Din F ud, Aman W, Ullah I, et al. Effective use of nanocarriers as drug delivery systems for the treatment of selected tumors. *International Jornal of Nanomedicine*. 2017;12:7291-7309.
159. Akbarzadeh A, Rezaei-Sadabady R, Davaran S, et al. Liposome: classification, preparation, and applications. *Nanoscale Research Letters*. 2013;8(1):102.
160. Meng S, Su B, Li W, et al. Integrin-targeted paclitaxel nanoliposomes for tumor therapy. *Medical Oncology*. 2011;28(4):1180-1187.
161. Deshpande PP, Biswas S, Torchilin VP. Current trends in the use of liposomes for tumor targeting. *Nanomedicine*. 2013;8(9):1509-1528.
162. Bangham AD, Horne RW. Negative staining of phospholipids and their structural modification by surface-active agents as observed in the electron microscope. *Journal of Molecular Biology*. 1964;8(5):660-668.
163. Bartlett GR. Phosphorus assay in column. *The Journal of Biological Chemistry*. 1959;234(3):466-468.
164. Veiga SR, Ge X, Mercer CA, et al. Phenformin-induced mitochondrial dysfunction sensitizes hepatocellular carcinoma for dual inhibition of mTOR. *Clinical Cancer Research*. 2018;24(15):3767-3780.
165. Vinci M, Gowan S, Boxall F, et al. Advances in establishment and analysis of three-dimensional tumor spheroid-based functional assays for target validation and drug evaluation. *BMC Biology*. 2012;10:29.
166. Baba M, Inoue M, Itoh K, Nishizawa Y. Blocking CD147 induces cell death in cancer cells through impairment of glycolytic energy metabolism. *Biochemical and Biophysical Research Communications*. 2008;374(1):111-116.
167. Frederick JW, Sweeny L, Hartman Y, Zhou T, Rosenthal EL. Epidermal growth factor receptor inhibition by anti-CD147 therapy in cutaneous squamous cell carcinoma. *Head & Neck*.

2016;38(2):247-252.

168. Miranda-gonçalves V, Granja S, Martinho O, et al. Hypoxia-mediated upregulation of MCT1 expression supports the glycolytic phenotype of glioblastomas. *Oncotarget*. 2016;7(29):46335-46353.

169. Pinheiro C, Longatto-Filho A, Pereira SMM, et al. Monocarboxylate transporters 1 and 4 are associated with CD147 in cervical carcinoma. *Disease Markers*. 2009;26(3):97-103.

170. Schneiderhan W, Scheler M, Holzmann K-H, et al. CD147 silencing inhibits lactate transport and reduces malignant potential of pancreatic cancer cells in in vivo and in vitro models. *Gut*. 2009;58(10):1391-1398.

171. Han T, Zhan W, Gan M, et al. Phosphorylation of glutaminase by PKCε is essential for its enzymatic activity and critically contributes to tumorigenesis. *Cell Research*. 2018;28(6):655-669.

172. DeBerardinis RJ, Cheng T. Q's next: the diverse functions of glutamine in metabolism, cell biology and cancer. *Oncogene*. 2010;29(3):313-324.

173. Yurchenko V, Constant S, Eisenmesser E, Bukrinsky M. Cyclophilin-CD147 interactions: a new target for anti-inflammatory therapeutics. *Clinical and Experimental Immunology*. 2010;160(3):305-317.

174. Grass GD, Tolliver LB, Bratoeva M, Toole BP. CD147, CD44, and the epidermal growth factor receptor (EGFR) signaling pathway cooperate to regulate breast epithelial cell invasiveness. *The Journal of Biological Chemistry*. 2013;288(36):26089-26104.

175. Grass GD, Dai L, Qin Z, Parsons C, Toole BP. CD147: regulator of hyaluronan signaling in invasiveness and chemoresistance. *Advances in Cancer Research*. 2014;123:351-373.

176. Muramatsu T. Basigin (CD147), a multifunctional transmembrane glycoprotein with various binding partners. *The Journal of Biochemistry*. 2016;159(5):481-490.

177. Yang S, Qi F, Tang C, et al. CD147 promotes the proliferation, invasiveness, migration and angiogenesis of human lung carcinoma cells. *Oncology Letters*. 2017;13(2):898-904.

178. Chen R, Wang SJ, Zhang Y, Hou R, Jiang JL, Cui HY. CD147 promotes cell motility via upregulation of p190-B RhoGAP in hepatocellular carcinoma. *Cancer Cell International*. 2016;16:69.

179. Amit-Cohen B-C, Rahat MM, Rahat MA. Tumor cell-macrophage interactions increase angiogenesis through secretion of EMMPRIN. *Frontiers in Physiology*. 2013;4:178.

180. Zhao M, Sun Y, Zhu X, et al. Antibody-targeted immunocarriers for cancer treatment. *Mini-Reviews in Medical Chemistry*. 2013;13(14):2026-2035.

181. Krishnamurthy S, Ng VWL, Gao S, Tan M, Yang YY. Phenformin-loaded polymeric micelles for

targeting both cancer cells and cancer stem cells in vitro and in vivo. *Biomaterials*. 2014;35(33):9177-9186.

182. Asakura T, Yokoyama M, Shiraishi K, Aoki K, Ohkawa K. Chemotherapeutic effect of CD147 antibody-labeled micelles encapsulating doxorubicin conjugate targeting CD147-expressing carcinoma cells. *Anticancer Research*. 2018;38(3):1311-1316.

183. Wang J, Wu Z, Pan G, et al. Enhanced doxorubicin delivery to hepatocellular carcinoma cells via CD147 antibody-conjugated immunoliposomes. *Nanomedicine*. 2018;14(6):1949-1961.

Chapter 8

ANNEX

8. ANNEX 1

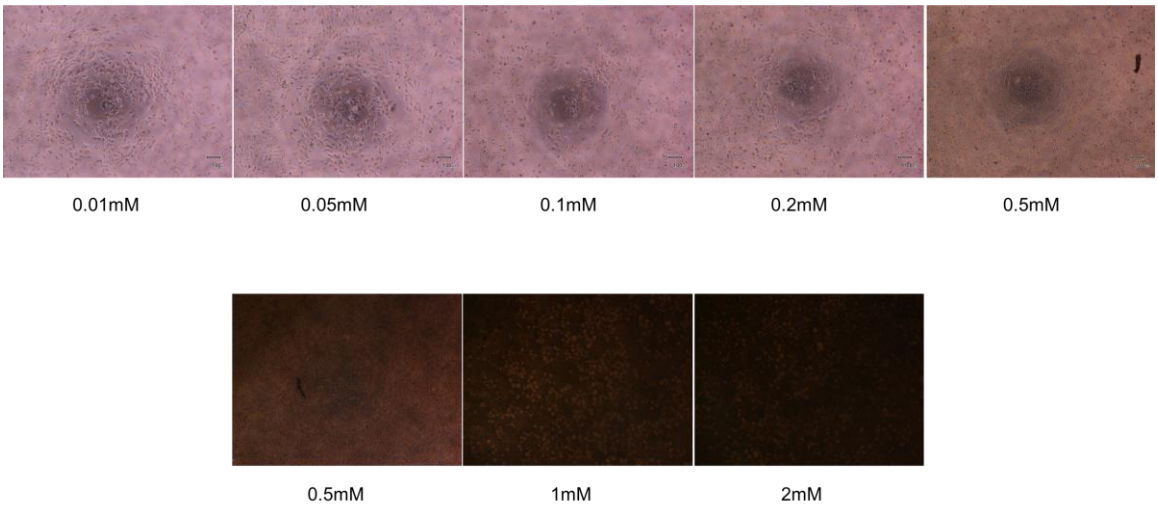

Figure 8.1. Liposomes from sample A (at the top) and from sample B (at the bottom). This figure shows representative images of lung cancer cells treated with different concentrations of liposomes from sample A or sample B. As mentioned in Chapter 4: Results – Section 4.6, we noted that the concentrations of liposomes from sample B were higher than expected. Images were taken under the Olympus IX51 microscope at 40x magnification.